DESIGN AND ANALYSIS OF DEFECTED GROUND STRUCTURE BAND PASS FILTER (DGS-BPF) FOR ENERGY HARVESTER APPLICATION

By

ALFRED ARVIND RAJ

FINAL REPORT PROJECT

Submitted to the Department of Electrical & Electronic Engineering

in Partial Fulfillment of the Requirements

for the Degree

Bachelor of Engineering (Hons)

(Electrical & Electronic Engineering)

Universiti Teknologi PETRONAS

Bandar Seri Iskandar

31750 Tronoh

Perak Darul Ridzuan

CERTIFICATION OF APPROVAL

DESIGN AND ANALYSIS OF DEFECTED GROUND STRUCTURE BAND PASS FILTER (DGS-BPF) FOR ENERGY HARVESTER APPLICATION

by

Alfred Arvind Raj

A project dissertation submitted to the
Department of Electrical & Electronic Engineering
Universiti Teknologi PETRONAS
in partial fulfillment of the requirement for the
Bachelor of Engineering (Hons)
(Electrical & Electronic Engineering)

Approved:

_____

(Mohd Azman Bin Zakariya)
Project Supervisor

UNIVERSITI TEKNOLOGI PETRONAS

TRONOH, PERAK

September 2013

CERTIFICATION OF ORIGINALITY

This is to certify that I am responsible for the work submitted in this project, that the original work is my own except as specified in the references and acknowledgements, and that the original work contained herein have not been undertaken or done by unspecified sources or persons.

_____

Alfred Arvind Raj

ABSTRACT

The living standards of our community nowadays have changed with the flow of advanced technology. A huge drastic growth in microwave communication has become a stepping stone for many researches to come out with several ideas for improvement in this field.

Band pass filter is one of the best examples of improvement in microwave communication. Many applications have been discovered by using band pass filter such as using Defected Ground Structure (DGS) in band pass filter.

In this paper, a microstrip band pass filter is proposed. The filter is designed and develops for energy harvester circuit which will be operating at 900 MHz band. Defected ground structure (DGS) parameters will be tuned to measure the performance of energy harvester circuit. The design technique will be verified by the result obtained.

This project will be done in stages and many steps involved for this project to be fully complete. The first stage would be the designing and fabrication of band pass filter according to it requirement which is operating at 900 MHz band. Then the second and the last stage is the interference of the filter with the energy harvester circuit.

The system was successfully integrated. The energy harvester circuit can be operated with the designed 900 MHz band pass filter using defected ground structure.

ACKNOWLEDGEMENTS

All praises be to God, for His help and guidance, I was able to complete my Final Year Project and write this Final Report Project.

I would like to offer my highest gratitude to my supervisor, Mr. Mohd Azman Bin Zakariya, Lecturer of Electrical & Electronic Engineering Department, Universiti Teknologi PETRONAS (UTP). His continuous guidance and supervision helped me during the past two semesters in completing my final year project. He provided me information and also concepts that I should understand in order to finish my project.

Besides that, I also would like to convey my deepest appreciation to my Graduated Assistant (GA), Mr. Talha Khan. He has been so helpful from the beginning till the end of this project completion. He guided me with care and teaches me how to handle difficult software and also the design simulation.

Finally, I would like to thank all my lecturers, colleagues, family and friends who supported me throughout this period of project completion.

TABLE OF CONTENTS

List of Figures

List of Tables

List of Abbreviations

Abbv	Definitions
DGS	Defected Ground Structure
BPF	Band Pass Filter
EBG	Electromagnetic Band Gap
DGSR	Defected Ground Stepped Resonator
SIR	Stepped Impedance Resonator
DSIR	Defected Stepped Impedance Resonator
CPW	Coplanar Waveguide
FYP I	Final Year Project 1
FYP II	Final Year Project 2
EHC	Energy Harvester Circuit
Tx	Transmitter
RF	Radio Frequency
LPF	Low Pass Filter

CHAPTER 1
INTRODUCTION

1.1 Introduction of Project

High achievement and stringent filtering structure are the major requirements of modern microwave communication systems. Nowadays, electromagnetic band gap (EBG) materials are the popular demand for applications in microwave and millimeter wave filters. These filters are using the defected ground structures (DGS) which is a generic structure. In order to improvise the stop and pass band structures, DGS cells have been continuously used in filtering circuits. The uncertainty response of microstrip low pass filters and coupled microstrip line band pass filters has led to the usage of DGS for the purpose of improvise and also for ready designed devices for example filters and couplers.

1.2 Problem Statement

In filter design there is a requirement of low ripple level and narrow bandwidth; while amplifiers design require high gain with compact size. The integration of DGS into filter design shows a potential to control the ripple level up to 0.01 % and also is able to tune to operate at narrow bandwidth of 200 MHz. In rectifier circuit design, the integration of DGS will be able to achieve high gain for the output. The size, harmonics suppression and efficiency of band pass filter for energy harvester circuit design can be improved with the help of proposed DGS. The performance and behavior of the proposed structure need to be analyzed.

1.3 Objective

The objective of this project is to design a Defected Ground Structure Band Pass Filter (DGS-BPF) with the following features:

- To operate at 900 MHz band.
- To perform analysis on tuning parameter of Defected Ground Structure (DGS) unit cell for tuning the Band Pass Filter (BPF).
- To measure the performance of energy harvester circuit design with integration of DGS-BPF.

1.4 Scope of study

In this project, fabrication of DGS – BPF filter will be required and it will be done in Printed Circuit Board (PCB) laboratory. Before that, the band pass filter will be simulated or designed using CST software, which is a high frequency computer simulation. The microstrip with and without DGS is tested and measured in RF microwave lab. The desired designed DGS-BPF is integrated with the energy harvester circuit to complete its application.

1.5 Relevancy of the Project

Many filter design has been done before with DGS but the application of it is not so clear. Through this project, the implementation or the application of DGS-BPF is shown so that a clearer view and understanding can be achieved. Hopefully it will be used more widely in the future for creating more applications which can ease and help in communication area or expertise. Besides that, many improvements also can be done in order to benefits the use of DGS-BPF.

1.6 Feasibility of the Project

This project was completed within 8 months or to be more specific within two semesters. This project is also successfully completed in the range of allocated budget which involve a prototype with circuits.

CHAPTER 2
LITERATURE REVIEW& THEORETICAL BACKGROUND

2.1 Literature Review

There are many researches has been done previously related to this topic or lead to this idea in my research paper. However most of the previous researches that have been done are not exactly focusing on the area of this investigation. Nevertheless, by reviewing previous research papers, many ideas were managed to be obtained to assist in this project paper.

Haiwen Liu et al. proposed an investigation on band pass filter with two-pole based on fractal shaped Defected Ground Stepped Resonator (DGSR)[1]. A modified fractal Hilbert curve resonator is shown in Figure 2.1(a). The spacing between the strips is 0.2 mm and the width of the strip is also 0.2 mm. Figure 2.1(b) shows a Hilbert fractal curve with defected ground structure resonator.

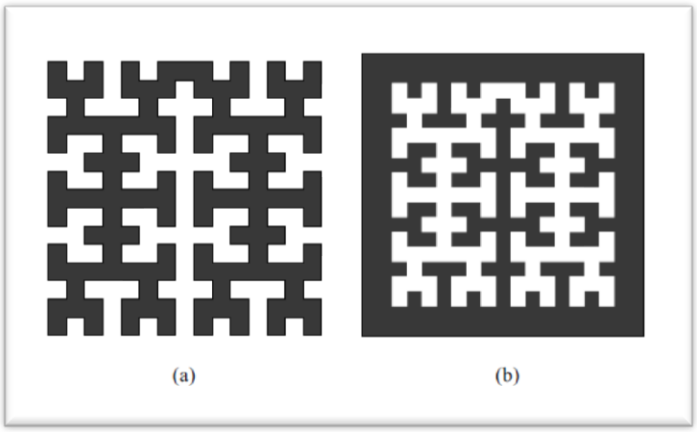

Figure 2.1: Fractal microstrip resonator and DGSR

A dual-band microstrip band pass filter also has been proposed in the previous research. [2]. Pai-Yi Hsiao et al. had applied a pair of half-wavelength open-loop resonators on the top layer and a symmetric bended squared stepped impedance resonator (SIR) on the bottom layer.

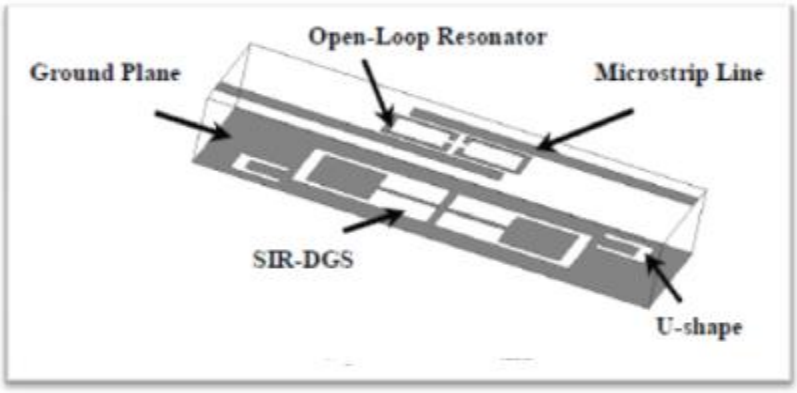

Figure 2.2: Dual-band filter

Chul-Soo Kim et al. has suggested the novel etched lattice shape as a defected ground structure (DGS). Different values of dimension have been used to investigate the changes in the effective inductance, capacitance, cutoff frequency and attenuation pole location.[3]

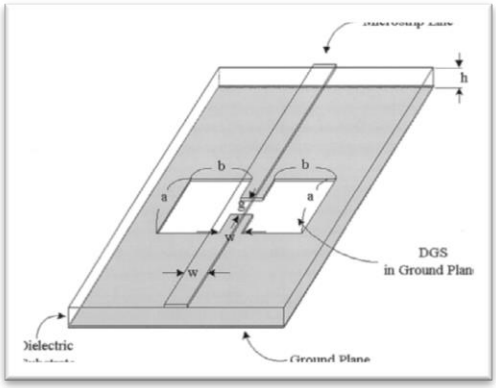

Figure 2.3: DGS unit lattice.

Table 1.1: DGS circuit parameter

	DGS dimensions		
	$a = b = 1.3$mm	$a = b = 2.5$mm	$a = b = 4.6$mm
Inductance (nH)	0.3675	0.865945	1.97725
Capacitance (pF)	0.51222	0.52845	0.537947
Cutoff Frequency (GHz)	10.15	6.085	3.62
Attenuation pole Location (GHz)	11.6	7.44	4.88

Table above shows the results of experiment. The values of inductance, capacitance, cutoff frequency and also attenuation pole location vary with the values of DGS dimension [3].

Bian Wu et al. proposed an idea of designing a dual-band filter based on defected stepped impedance resonator (DSIR). The frequency that was used to operate is 1.85 GHz and 2.35 GHz[4]. Figure 2.4 shows the geometry of the proposed defected stepped impedance resonator (DSIR) and the stepped impedance resonator (SIR) [4].

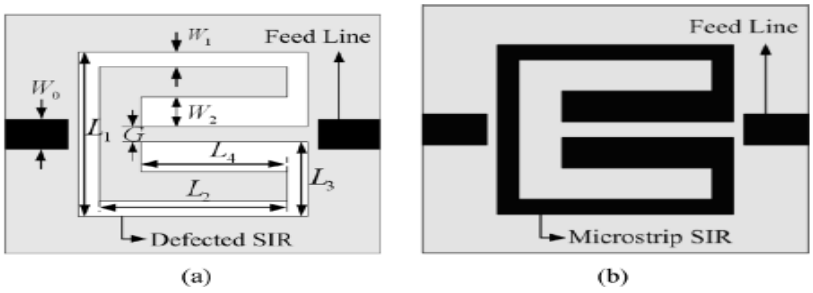

Figure 2.4: Structure of defected and microstrip SIR unit.

Vesna Radisic et al. has proposed a new two-dimensional (2-D) photonic band gap (PBG) structure that does not require any drilling process and only partial etching of the ground plane with different circle radii[5].

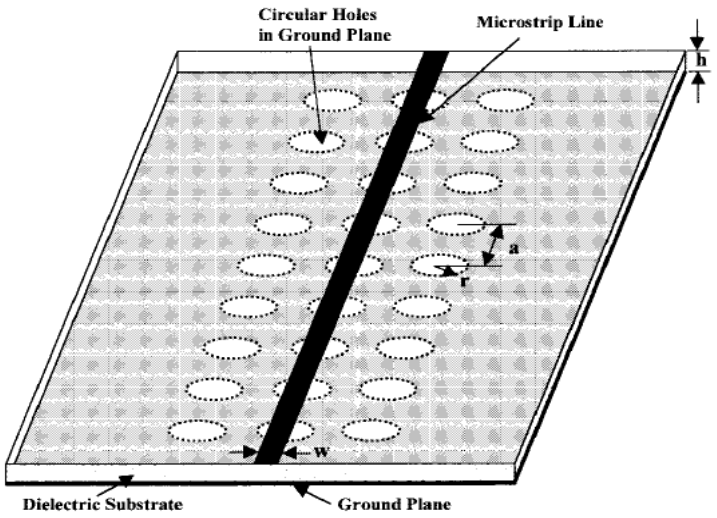

Figure 2.5: Square PBG structure.

Heba B. El-Shaarawy et al. has done some investigation on a reconfigurable DGS cell for multi-stop band filter on Coplanar Waveguide (CPW) technology. Three different frequencies have been tested which are 2.28 GHz, 7.44 GHz and 9.85 GHz[6].

Sachin Singh and Banmali Rawat proposed a new stepped impedance resonator (SIR) with new configuration of defected ground structure (DGS) that is fabricated on anisotropic and isotropic[7].

A new compact 2D defected ground structure (DGS) which is based on a 1D DGS was studied by H. Liu et al[8]. Sio-Weng Ting et al. suggested compact microstrip quasi-elliptical band pass filter using open-loop dumbbell shaped defected ground structure (DGS). This is a quasi-elliptic band pass and bounded by two transmission zeros[9].

2.2 Theoretical Background

A filter can be defined as a two port network which controls the frequency response at a certain point in a microwave system. Nowadays, microstrip is used to design filter. It is a type of electrical transmission line which is used to convey microwave frequency signals. It consists of substrate which is from a ground plane by a dielectric layer and this is known as periodic structure [10].

Every unit cells consists of length (d) and the susceptance (b) which is normalized to the impedance (z_0). The relationship between voltages and currents are as per below using matrix.

$$\begin{bmatrix} Vn \\ In \end{bmatrix} = \begin{bmatrix} A & B \\ C & D \end{bmatrix} \begin{bmatrix} Vn+1 \\ In+1 \end{bmatrix} \tag{2.1}$$

In normalized form:

$$\begin{bmatrix} A & B \\ C & D \end{bmatrix} = \begin{bmatrix} \cos\frac{\theta}{2} & j\sin\frac{\theta}{2} \\ j\sin\frac{\theta}{2} & \cos\frac{\theta}{2} \end{bmatrix} \begin{bmatrix} 1 & 0 \\ jb & 1 \end{bmatrix} \begin{bmatrix} \cos\frac{\theta}{2} & j\sin\frac{\theta}{2} \\ j\sin\frac{\theta}{2} & \cos\frac{\theta}{2} \end{bmatrix}$$

$$= \begin{bmatrix} \left(\cos\theta - \frac{b}{2}\sin\theta\right) & j\left(\sin\theta + \frac{b}{2}\cos\theta - \frac{b}{2}\right) \\ j\left(\sin\theta + \frac{b}{2}\cos\theta + \frac{b}{2}\right) & \left(\cos\theta - \frac{b}{2}\sin\theta\right) \end{bmatrix} \tag{2.2}$$

2.2.1 Stripline

There are two conducting ground planes of separation *b* centered with a thin conducting strip of width W in the strip transmission line. This entire region is filled with a dielectric of relative permittivity. Stripline support Transverse Electromagnetic (TEM) waves which is the required mode of operation. This is because it consists of two conductors and a homogenous dielectric [11].

$$Z_o = \sqrt{\frac{L}{C}} = \frac{\sqrt{LC}}{C} = \frac{1}{v_p C} \tag{2.3}$$

Where L and C are the inductance and capacitance per unit length of the line.

2.2.2 Microstrip line

The basic mode of propagation of microstrip line is not a pure TEM mode. The dielectric region contains most of the field lines and some in the air region above the substrate. The phase velocity and propagation constant are given by as below [11].

$$V_p = \frac{C}{\sqrt{\varepsilon_e}} \tag{2.4}$$

The effective dielectric constant is given by:

$$\varepsilon_e = \frac{\varepsilon_r + 1}{2} + = \frac{\varepsilon_r - 1}{2} \frac{1}{\sqrt{1+12d/W}} \tag{2.5}$$

Where,

$$1 < \varepsilon_e < \varepsilon_r$$

2.2.3 CST Microwave Tutorial

This is one of the software that will be used to design microstrip band pass filter. In order to learn how to use this software, we have to go through its tutorial and the tutorial is as per below.

a) Filter Tutorial

This tutorial will help to learn how to simulate planar devices such as a Narrow Band Filter.

i) Select a template

Here, the Resonator template should be selected once CST is started. The units will automatically be set to mm and GHz with the background material to be perfect electrically conducting. Before starting the modeling process, the working planes should be set and the sizes must be large enough for the device.

ii) Draw the filters housing

The interior of the filter need to be modeled whereas the exterior of the filter does not need to be modeled because the background material has been set to electric. The structure modeling should be started by entering the filters housing which is by creating an air-brick. Next the coordinates for X-plane, Y-plane and the height have to be inserted. It is better to switch display to wireframe mode as the structures will be inserted into air brick and this will cause the shapes to be hidden inside the brick.

iii) Create the cylindrical resonators

Next is to create the cylindrical resonators inside the air brick. The first step in this process is to enter the center point coordinates. The material of the cylindrical should be verified before continuing with the same procedure for the second cylinder. The second step is to create the iris between the two cavities. The procedure is same with the creation of the air brick above.

iv) Create the coaxial couplings

At this point, the filters internal structure has been modeled; however the next step will be the coaxial coupling modeling on both side walls of the filter. First, the working coordinate system should be aligned with one of the side walls of the filter. This procedure should be carried out first before begin modeling the cylinders because it will allow to model the coupling structure in a more convenient way. Next the substrate material should be defined.

Till this point, one coaxial coupler has been modeled, but still need to create the second coupler. The second coupler can be easily achieved by creating a mirrored copy using a shape transformation. The coordinates of the second coupler should be opposite the first one in order to gain an exact coupler.

v) Define ports

Now the ports to the filter need to be added for which the S-parameters will be calculated. An infinitely long waveguide will be simulated by each port that is connected to the structure at the port plane. Waveguide ports will be used here as it is the most accurate way to calculate the S-parameters of filters. The port must cover the coaxial cable substrate completely because a waveguide port is based on the two dimensional mode patterns in the waveguides cross-section. Therefore two ports with same characteristics will be designed here.

vi) Define boundary conditions and symmetries

The structure is embedded in a perfect electrically conducting housing which means all boundaries are set to electric. In order to force the solver to calculate only the modes that has no tangential magnetic field, the symmetry plane YZ is set to magnetic. Next an appropriate frequency range is defined.

vii) S-parameter calculation

This is the final part or step in designing filter. Here, the filter device will be analyzed with three method; transient solver, frequency domain solver: general purpose, and resonant: fast S-parameter. The S-parameters are calculated with a hexahedral mesh, while the second simulation is performed with the tetrahedral mesh. The Narrow Band Filter is simulated.

CHAPTER 3
METHODOLOGY

3.1 Research Methodology

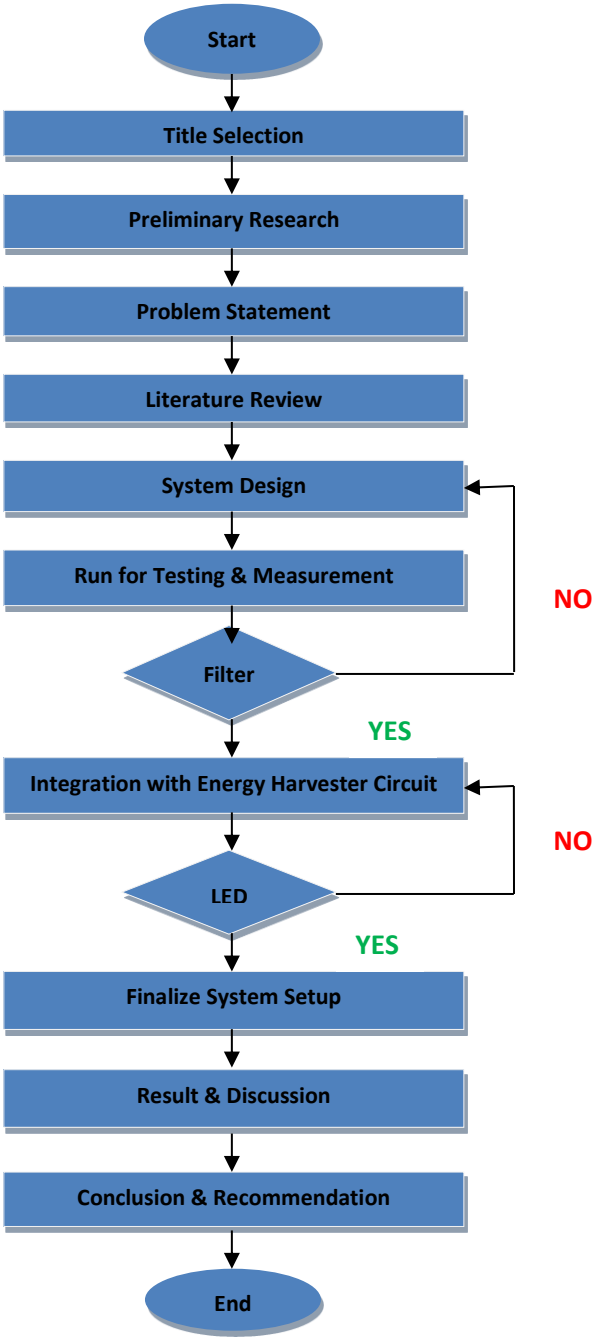

Figure 3.1: Research methodology flow chart

The first part is the development of the circuit design. In this part, the filter is designed using software. All the required measurement and parameters was inserted in order to get the required and accurate results. Next the designed filter is tested to check whether it functions as designed.

Once the result obtained is satisfied then the designed is saved in Gerber file format and sent for fabrication to proceed for further process. However, if the result obtained from the test run is not satisfied, then the overall process have to be repeated again with some changes in the parameters and also measurement that has been inserted.

The second part is the hardware processing part in which the design is fabricated. Once the designed filter is fabricated, it is sent to the lab to be tested and measured for the required values.

After it has passed the entire standard requirement, then the filter is tested again but this time with real life problem in order to confirm its sustainability. But if the filter failed to pass the standard requirement, then the process of fabrication plus with the designing process have to be carried out again until the desired values is obtained. If there is no error, then the filter is ready to be used.

Next, the designed filter is used to integrate with the energy harvester circuit. Three types of energy harvester circuits were used to test with the band pass filter. The first type is with band pass and also low pass filter which was already embedded in the energy harvester circuit. The second type is only with the low pass filter and the last type is without any internal filters, just the band pass filter which has been integrated with.

Lastly, all the results and readings obtained were collected and tabulated in order to represent it in a clearer view and for better understandings.

3.2 Block Diagram

3.2.1 Software

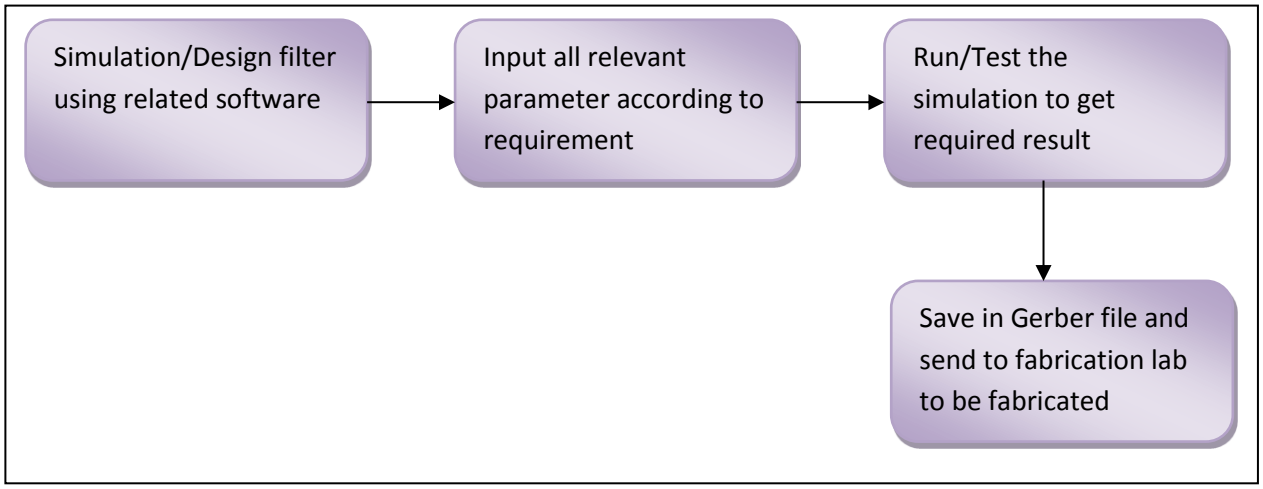

Figure 3.2: Simulation process of project for DGS-BPF

3.2.2 Hardware

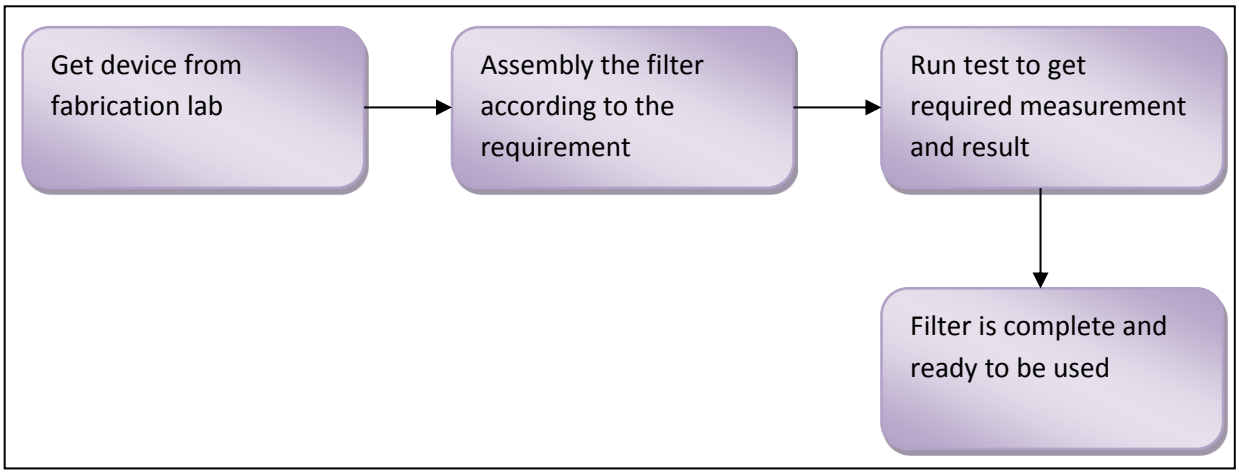

Figure 3.3: Fabrication process of project for DGS-BPF

3.3 Overall System Process

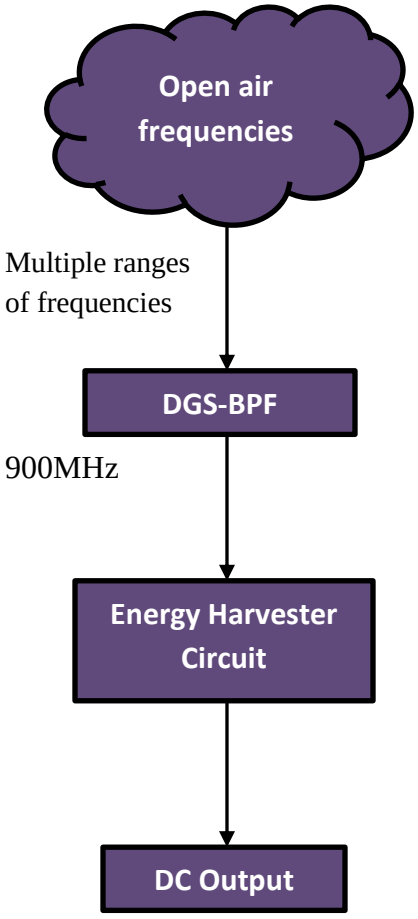

Figure 3.4: Overall system process

3.4 Gantt Chart & Milestone

3.4.1 Final Year Project I

Table 3.1: Final Year Project I Gantt Chart

FINAL YEAR PROJECT I														
No	**Activities**	**Week**												
		1	2	3	4	5	6	7	8	9	10	11	12	13	14
1	Title Selection														
2	Preliminary Research &Literature review														
3	Explore & Design BPF in CST Software														
4	BPF Fabrication														
5	Testing & Measurement of BPF														

Final Year Project I Milestones:

- Completion of title selection : Week 1
- Completion of preliminary research & literature review : Week 6
- Completion of BPF design in CST Software : Week 8
- Completion of BPF fabrication : Week 10
- Completion of testing & measurement of BPF : Week 14

3.4.2 Final Year Project II

Table 3.2: Final Year Project II Gantt Chart

FINAL YEAR PROJECT II														
No	**Details**	**Week**												
		1	2	3	4	5	6	7	8	9	10	11	12	13	14
1	Filter Test														
2	Filter Setup & Measurement														
3	Results Analysis														
4	Discussion														
5	Conclusion														

Final Year Project II Key Milestones:

- Completion of Filter Test : Week 4
- Completion of Filter Setup & Measurement : Week 9
- Completion of Analysis of Results : Week 10
- Completion of Discussion : Week 12
- Completion of Conclusion : Week 14

3.5 Tools

1) Software

- CST Microwave Studio
- Ansoft Designer

2) Hardware

- PCB fabrication
- Antenna
- Energy harvester circuit
- Connectors
- Frequency generator
- Coaxial cable
- Soldering tools

CHAPTER 4
RESULTS & DISCUSSION

This project consists of two main parts. The first part is the filter designing and the second part is the integration of band pass filter-defected round structure with the energy harvester circuit. Each part will be discussed in detail below.

4.1 Overview of Defected Ground Structure (DGS)

One of the new concepts that were applied to distribute microwave circuits is by Defected Ground Structure (DGS) technique. This is done by modifying the ground plane metal of a microstrip circuits intentionally to enhance performance. DGS allows placing a notch almost anywhere. It will disturb the shield current distribution in the ground plane and this disturbance will change characteristics of a transmission line such as line capacitance and inductance. Thus, when it placed just outside a band pass filter's pass band, the steepness of the rolloff and the close-in stop band are both improved. The need for a more complex design can be avoided if DGS elements are used to improve the stop band performance, because simple microstrip filters have a symmetrical stop bands.

For the testing and learning purposes, a 2400 MHz band pass filter with and without DGS was designed and simulated. The result of the testing is as per below.

a) Filter without DGS slot

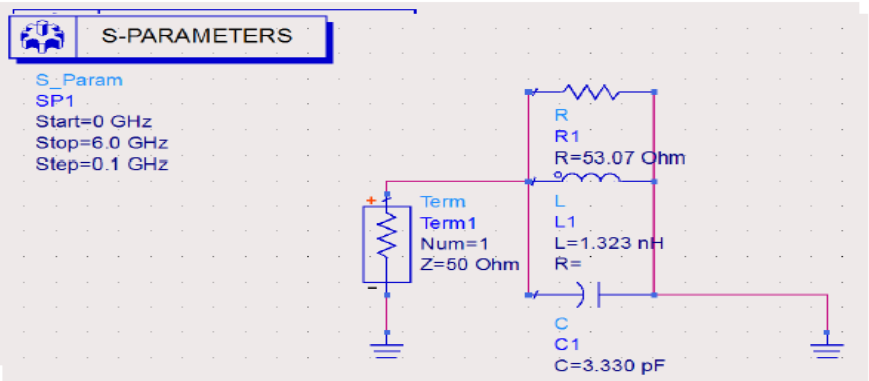

Figure 4.1: 2400 MHz band pass filter without DGS equivalent circuit

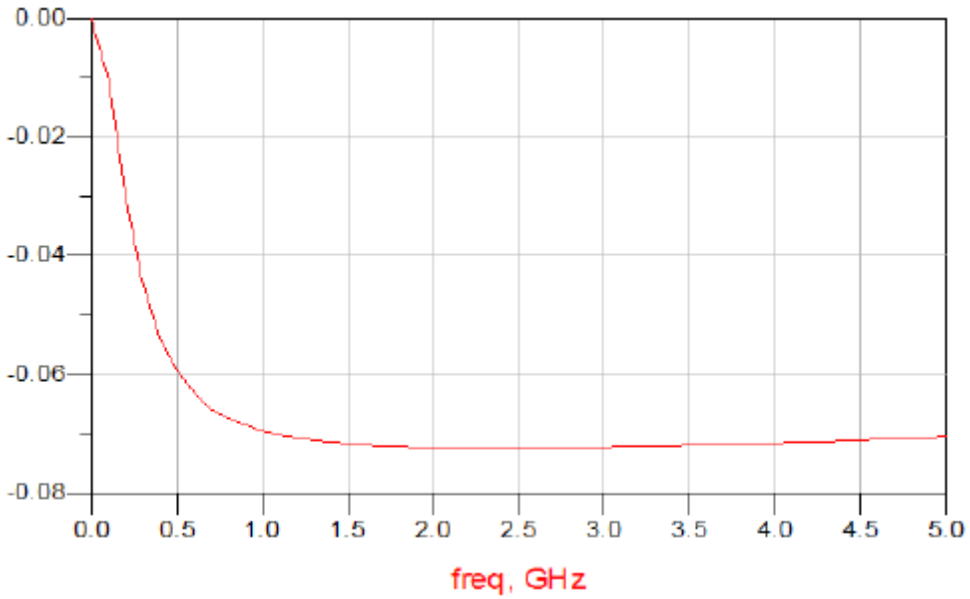

Figure 4.2: Presence of unwanted second harmonic

b) Filter with DGS slot

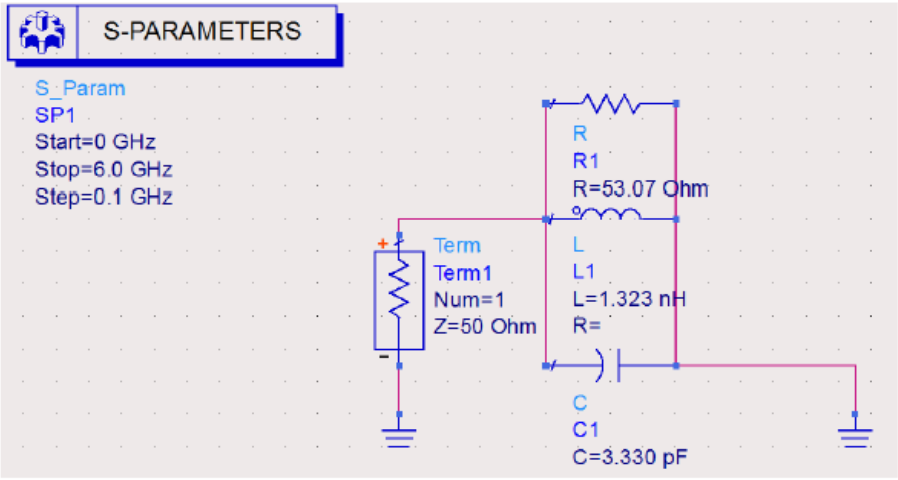

Figure 4.3: 2400 MHz band pass filter with DGS equivalent circuit

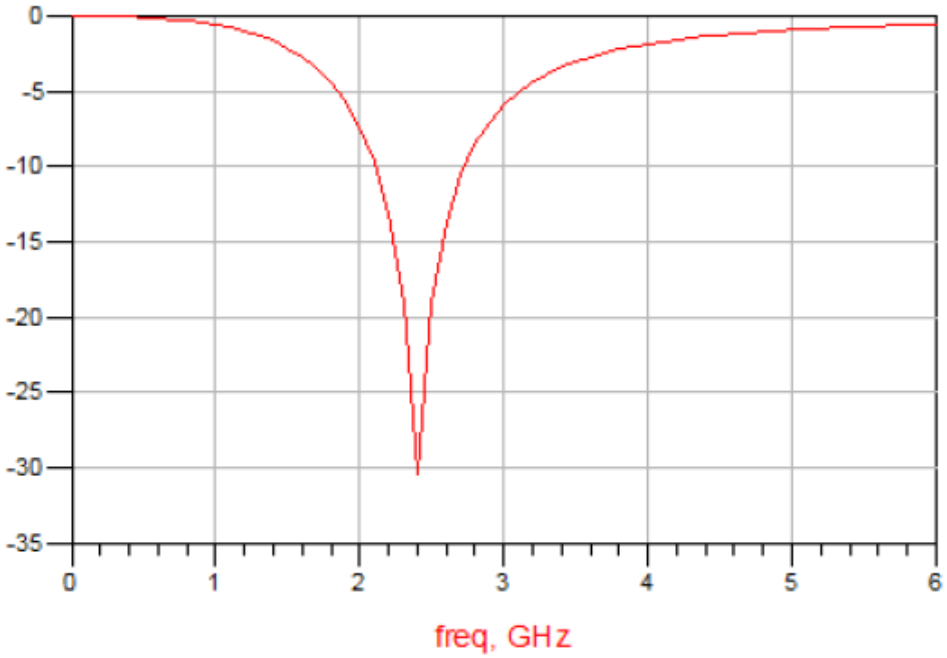

Figure 4.4: The resonance is at 2400 MHz with DGS slot and no unwanted second harmonic

Figure 4.1 and 4.3 shows the equivalent circuit for 2400 MHz band pass filter with and without DGS. The same value of R, L and C is used in order to show changes due to insertion of DGS only and not by other parameters. From the figure above it clearly state that when a DGS is used, the unwanted resonance is eliminated and it enhance the stop band of the filters.

4.2 Filter Designing

The same band pass filter with defected ground structure is simulated using CST Software. The parameters of the DGS are tuned in order to get the desired frequency. The frequency that was set in this step was 2400 MHz. The changes in S_{11} and S_{21} parameters are observed. Low pass prototype is transformed to a band pass response using frequency transformation formula.

Equations for band pass transformation

$$f = \frac{\text{fc}}{FBW}\left(\frac{\omega}{\omega 0} - \frac{\omega 0}{\omega}\right) \tag{4.1}$$

$$\text{FBW} = \frac{\omega 2 - \omega 1}{\omega 0} \tag{4.2}$$

$$\omega o = \sqrt{\omega 1 \omega 2} \tag{4.3}$$

Where $\boldsymbol{\omega 0}$ is the centre angular frequency and **FBW** is defined as the fractional bandwidth and $\boldsymbol{\omega 1}$ $\boldsymbol{\omega 2}$ are the pass band edge angular frequencies.

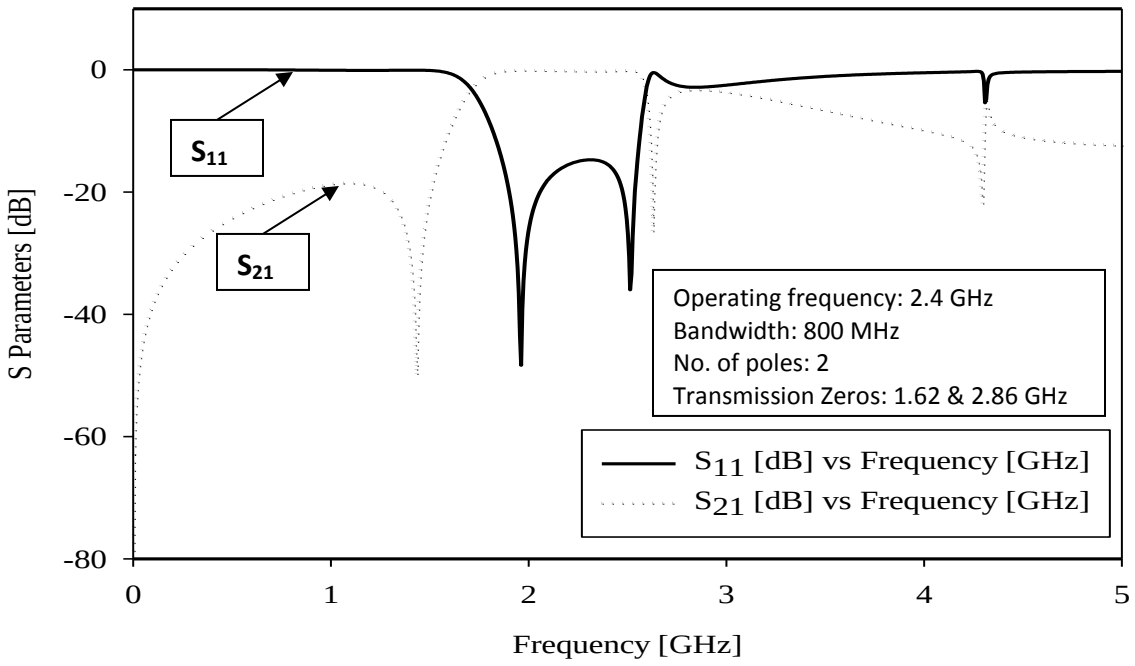

Figure 4.5: Simulation result of S_{11} and S_{21} parameter

Figure 4.5 shows the parameters that can be obtained from the simulated graph which can be inserted in the formula to be calculated. The value of $\boldsymbol{\omega 1}$ $\boldsymbol{\omega 2}$ can be obtained from the simulated result. Later the difference between the values will be divided with $\boldsymbol{\omega 0}$. The filter clearly shows two transmission poles and the transmission zeros are 1.62 GHz and 2.86 GHz

4.2.1 Comparison of the simulated result and measured result

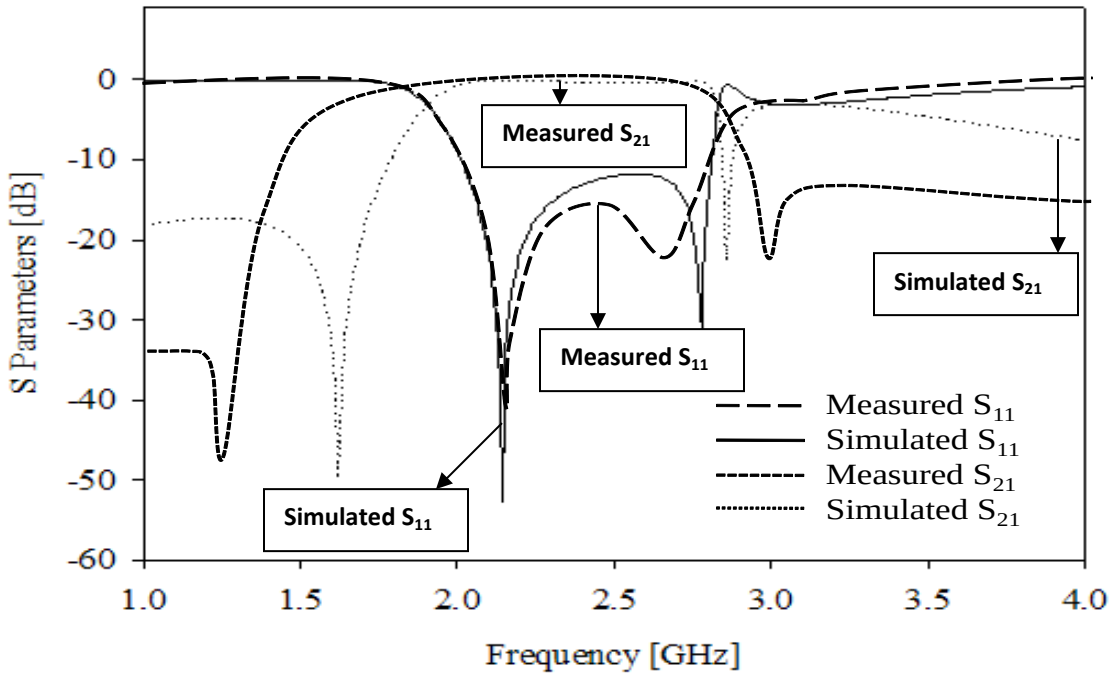

Figure 4.6: S_{11} and S_{21} parameters difference for band pass filter design

Figure 4.6 illustrate the comparison of the simulated and measured result. There are some slight deviations in the value of measured S_{11} and simulated S_{11}. But with the small deviation the result is still accepted as the value cannot affect the frequency. With this, it can be concluded that the simulated result and the measured result are same.

4.3 Tuning Parameter

The parameters of the simulated DGS were tuned in order to find the relationship with the result obtained.

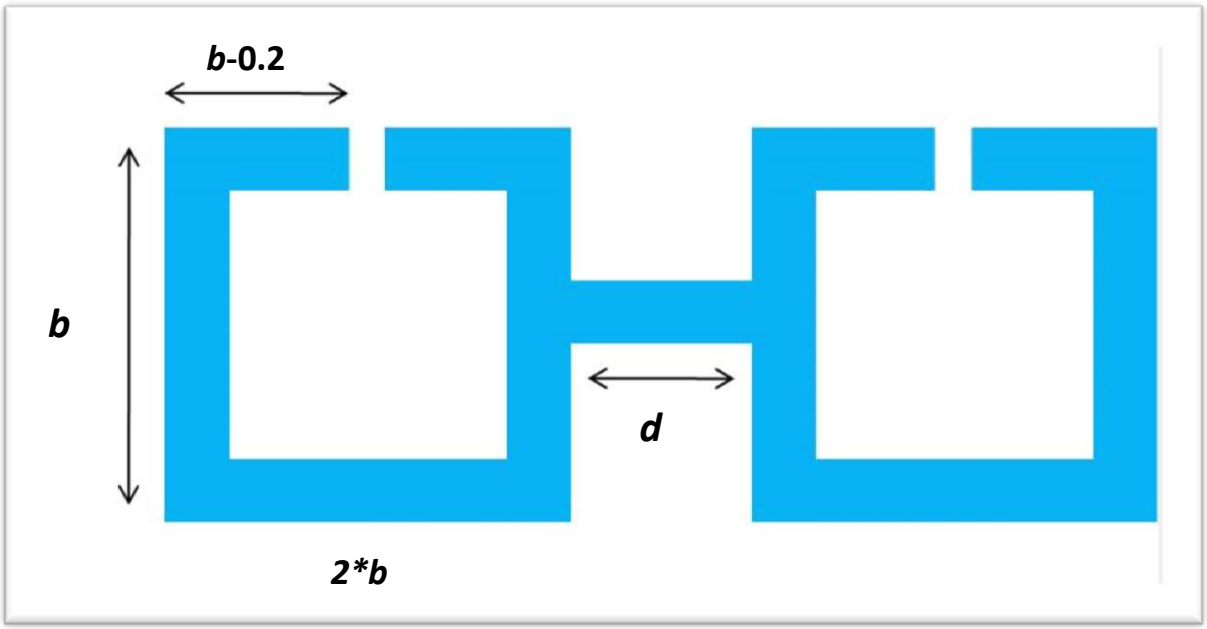

Figure 4.7: Dumbbell shaped DGS

Figure 4.7 shows the parameters that were used to tune in order to understand the relationship with the S_{11} and S_{21} result. The value of *b*, *2*b*, *b-0.2*, and *d* were tuned to see the changes obtained in the simulated result. Below is the original value for each parameter before it is tuned.

b = 6.0 mm
*2*b* = 12.0 mm
b-0.2 = 5.8 mm
d = 6.0 mm

4.3.1 Effects on Parameter *b*

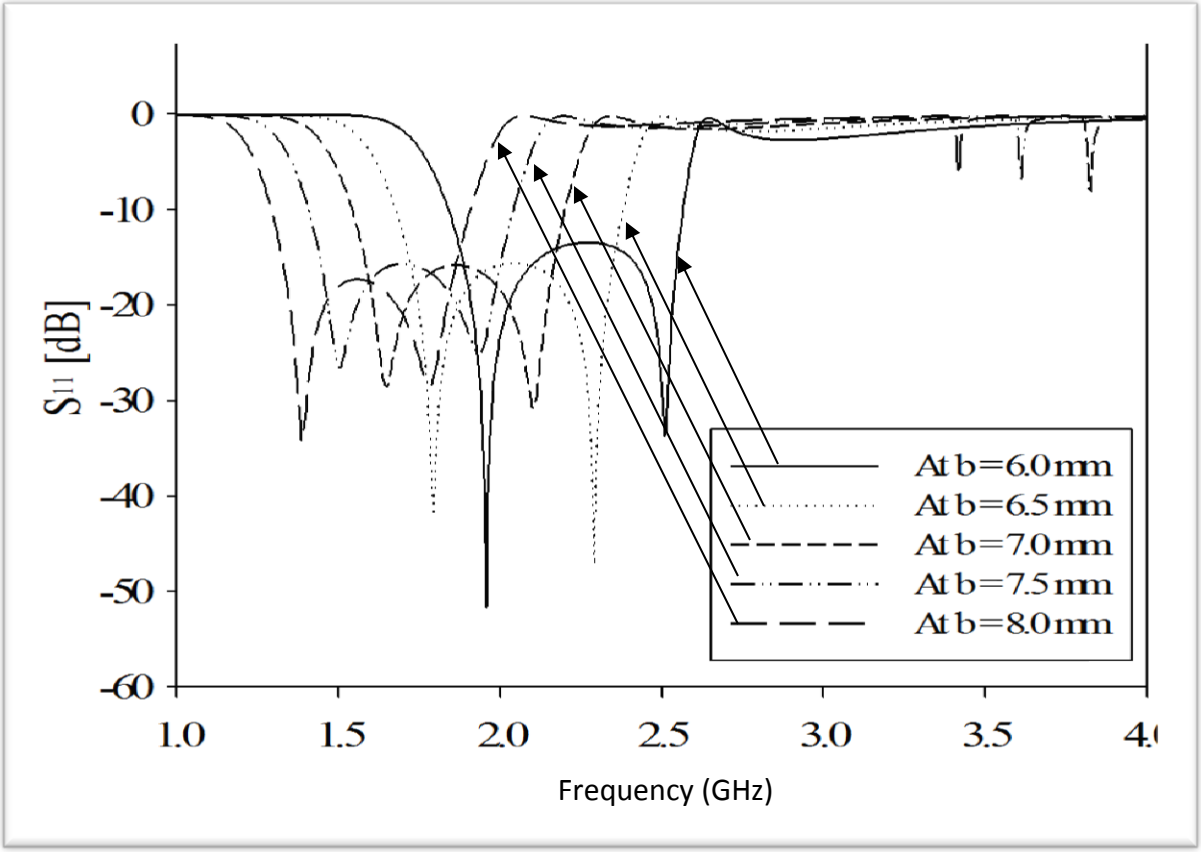

Figure 4.8: Changes in S_{11} and S_{21} parameters due to changes in value of *b*

Figure 4.8 shows the effects on the simulated graph when parameters *b* was changed from 6.0 mm to 8.0 mm. By increasing *b*, the centre frequency down shifts to lower frequency. Centre frequency is gradually changed from 2.23 GHz to 1.55 GHz for *b* = 6.0 mm to 8.0 mm, providing wide frequency of 0.68 GHz. The figure above concludes that by changing parameter *b*, the centre frequency will be affected.

4.3.2 Effects on Parameter 2*b*

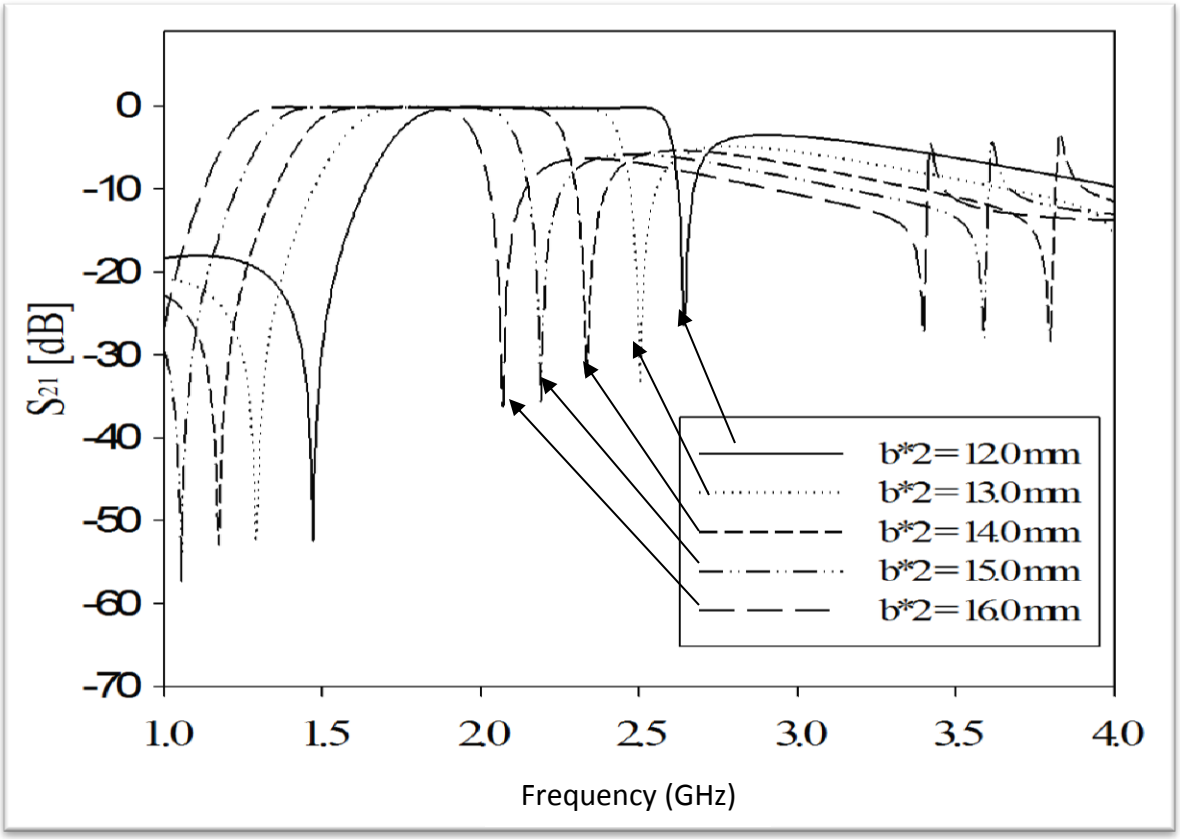

Figure 4.9: Changes in S_{11} and S_{21} parameters due to changes in value of 2*b

Figure 4.9 illustrate the changes of the location of the transmission zeros. By increasing 2*b from 12.0 mm to 16.0 mm, the location of lower and upper transmission zeros shifts downwards. It is down shifted from 1.46 GHz to 0.953 GHz and 2.64 GHz to 2.069 GHz. This proves that by changing the value of 2*b, the location of transmission zeros will be affected too.

4.3.3 Effects on Parameter *b*-0.2

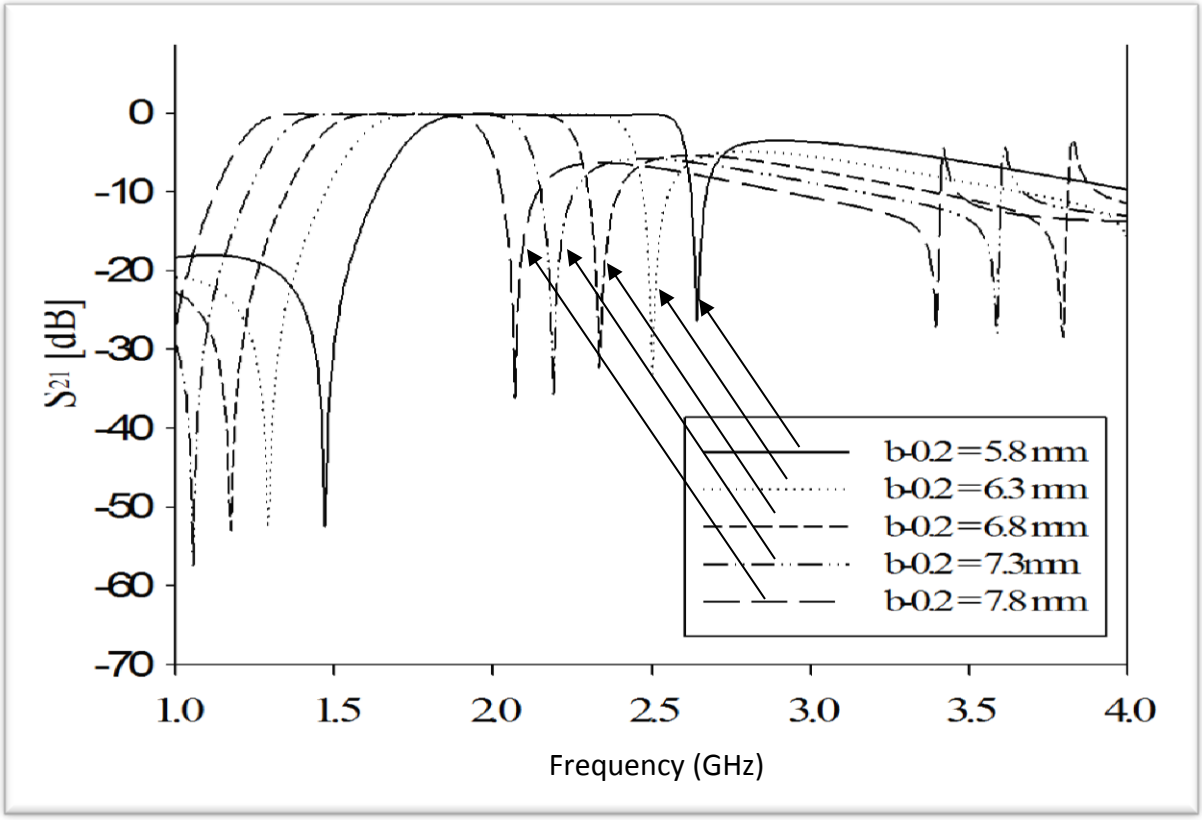

Figure 4.10: Changes in S_{11} and S_{21} parameters due to changes in value of *b*-0.2

Figure 4.10 shows the effects of changing the value of *b*-0.2. The effects are similar to the parameter 2**b*. The location of transmission zeros were shifted downwards by increasing the value of *b*-0.2. It is down shifted from 1.46 GHz to 0.953 GHz and 2.64 GHz to 2.069 GHz. This proves that the location of transmission zeros is influenced by the value of *b*-0.2 parameters.

4.3.4 Effects on parameter *d*

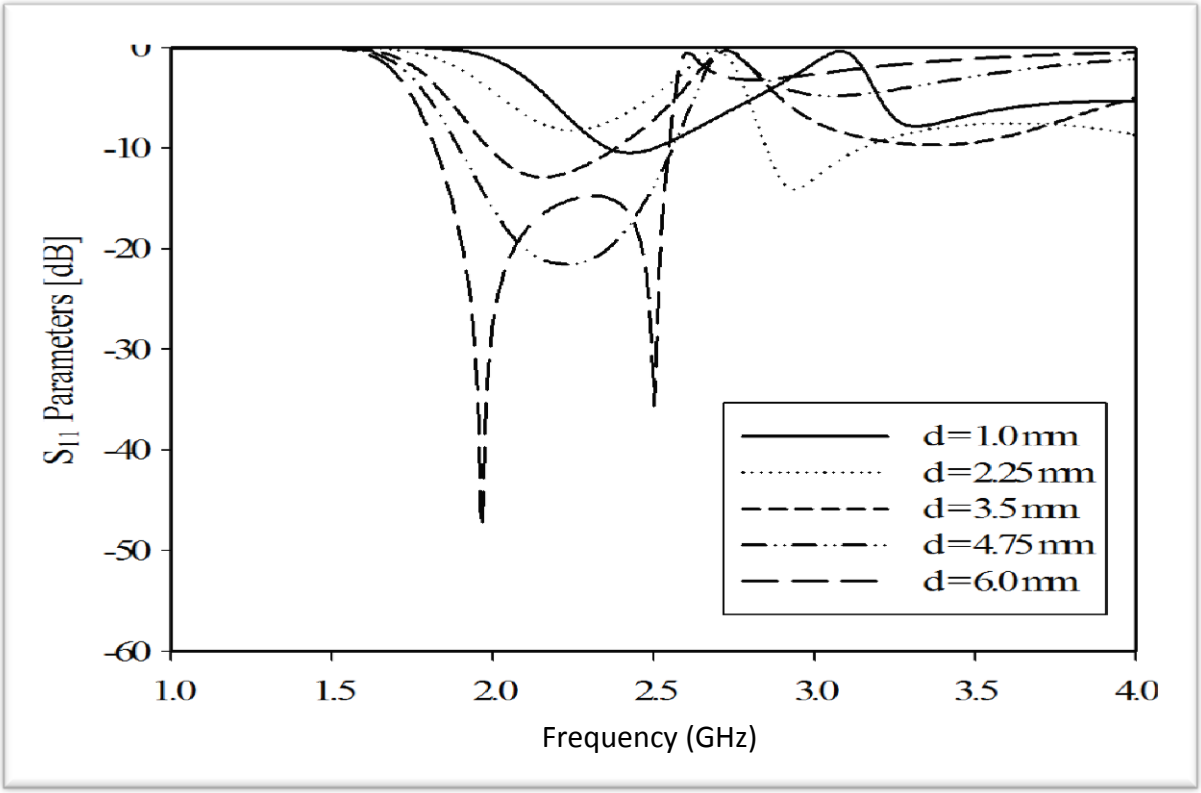

Figure 4.11: Changes in S_{11} and S_{21} parameters due to changes in value of d

Figure 4.11 shows the effect of parameter *d*. When the value of *d* is decreased beyond a certain limit, the band pass filtering characteristics loses. If the parameter *d* is decreased beyond 6.0 mm, the filter loses the attenuation pole. From the figure above, it can be concluded that, the band pass filtering characteristics is affected when the parameter *d* is changed. From the result that was obtained through parameter changes, it can be concluded as per table below.

Table 4.1: Summary of changes in tuning parameters

Parameter Changes	Results
Effects on *b*	Change in centre frequency
Effects on *b*-0.2	Change in location of transmission zeros
Effects on 2**b*	Change in location of attenuation poles
Effects on *d*	Change in bandwidth and band pass characteristics

Based on the Table 4.1, it is understood that any changes in these four parameters will affect the results obtained in S_{11} and S_{21}. A change in *b* affects the centre frequency. Therefore, in order to tune for 900 MHz, the length of *b* need to be changed further more. The other parameters were kept constant as it does not influence much in the objective of this project.

4.4 Filter Design

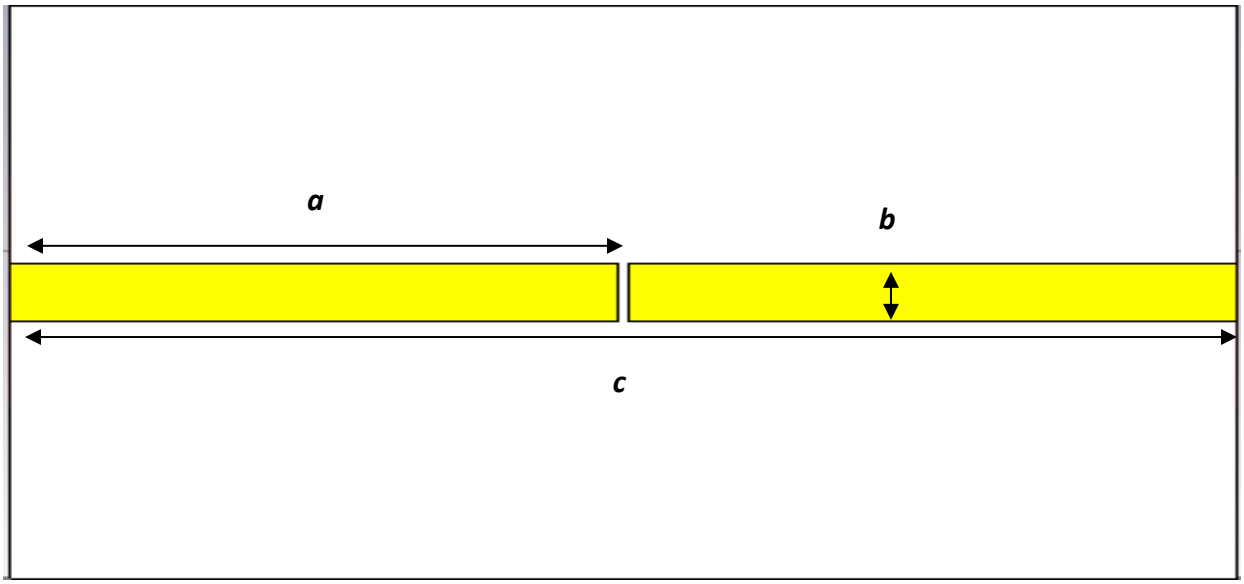

Figure 4.12: Front view of 900 MHz band pass filter with DGS

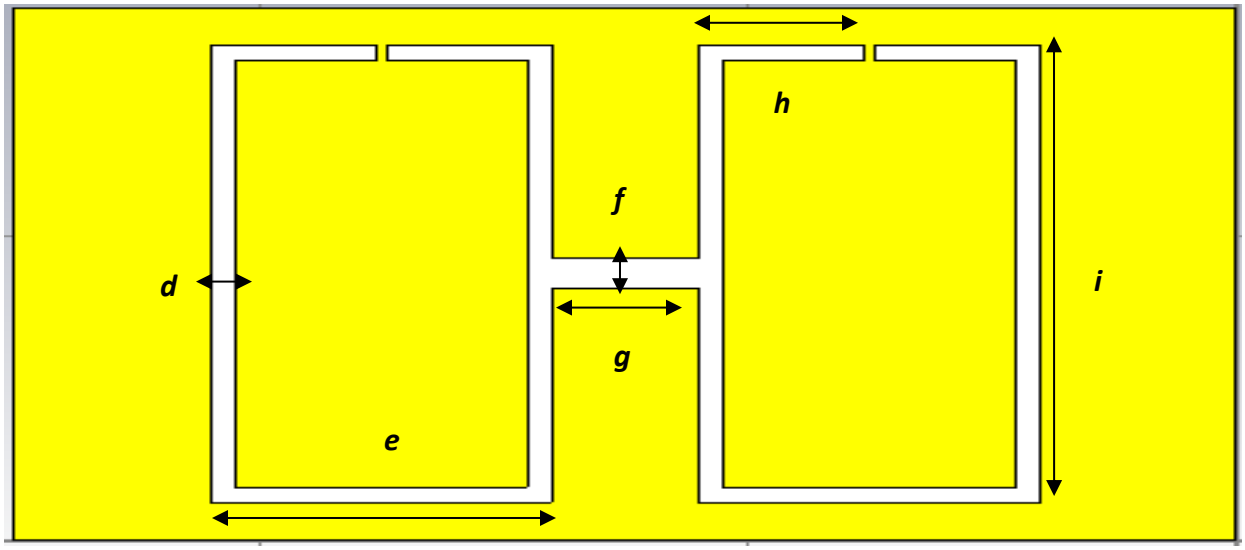

Figure 4.13: Back view of 900 MHz band pass filter with DGS

The ground is made of Rogers RT5800 lossy substrate and the other parts are made of copper annealed (lossy metal). The measurements for the filter are *a*= 9.8 mm, *b*=1.2 mm, *c*=20 mm, *d*=0.6 mm, *e*=8 mm, *f*=0.8 mm, *g*=1.5 mm, *h*=3.8 mm, *i*=10 mm. The x-length and y-length of the substrate is 22 mm and 12 mm respectively. The height of the substrate is 0.787 mm and height for the ground is 0.0175 mm. Both of the measurements are kept fixed in order to get a better reading.

From the testing progress for 2.4 GHz, it is clearly proven that by changing the length of DGS, the centre frequency is affected. Thus, in order to get 900 MHz of centre frequency, the length, *i*, is varied gradually. The pattern of the readings is shown in Table 4.2.

Table 4.2: Changes in tuning parameters for 900 MHz

h (mm)	f_c (GHz)	C_p (pF)	L_p (nH)
6.50	1.582	1.2461	6.812
6.75	1.524	1.2985	5.327
7.00	1.497	1.3121	4.671
7.25	1.413	1.3864	3.739
7.50	1.375	1.4375	2.314
7.75	1.302	1.4997	1.876
8.00	1.294	1.5312	0.945
8.25	1.225	1.5872	0.882
8.50	1.196	1.6691	0.803
8.75	1.132	1.7013	0.763
9.00	1.094	1.7842	0.663
9.25	1.056	1.8221	0.591
9.50	1.003	1.8896	0.437
9.75	0.979	1.9217	0.296
10.00	0.901	1.9766	0.218

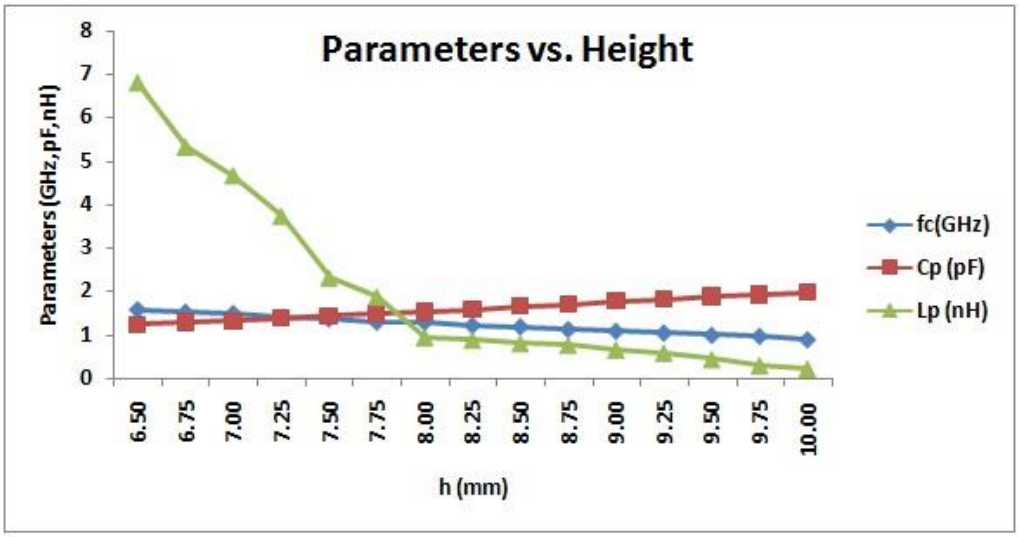

Figure 4.14: Graph of tuning parameters for 900 MHz

Table 4.2 shows the changes in the length of DGS that was tuned to get 900 MHz. The length of parameter *i* need to be increase gradually until the desired centre frequency is obtained which is 900 MHz. The trend for all the parameters has been plotted in a graph as shown in Figure 4.14

The simulation is later measured for S_{11} and S_{21} parameters before fabricated and below is the result obtained. The result obtained was the desired result which is with the centre frequency ranges from 900 MHz to 950 MHz and bandwidth of 0.2 GHz. Figure 4.15 shows the simulated result.

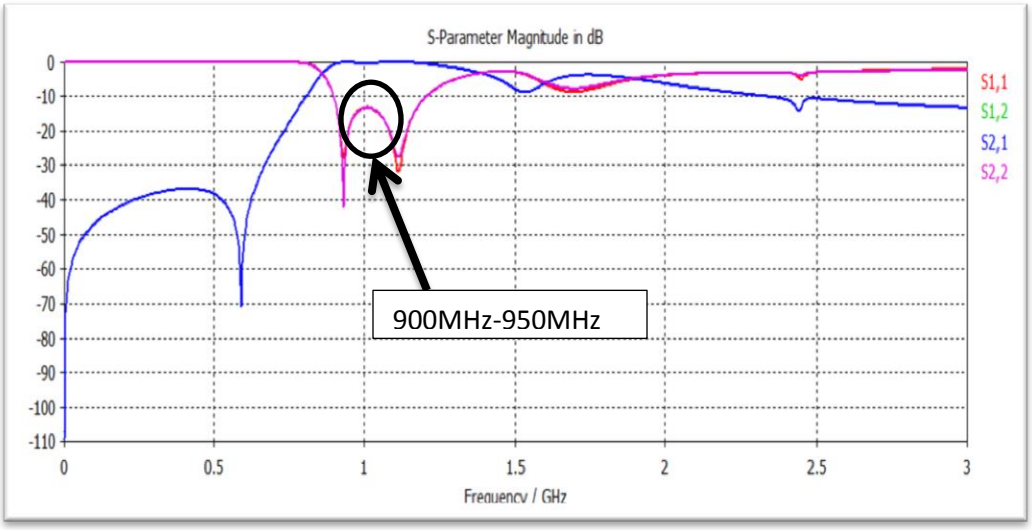

Figure 4.15: Simulated result for 900 MHz band pass filter with DGS

Figure 4.15 shows the S_{11} and S_{21} result obtained after the DGS is tuned for 900 MHz. It also shows two transmission poles with the bandwidth differences that can also be obtained through the graph.

4.4.1 Filter Fabrication

The simulated filter is sent to PCB lab for fabrication based on the parameters tuned in CST Software. Once the filter is fabricated, it is attached with connectors through soldering at both sides of its designed port. Figure below is the picture of the fabricated band pass filter with DGS.

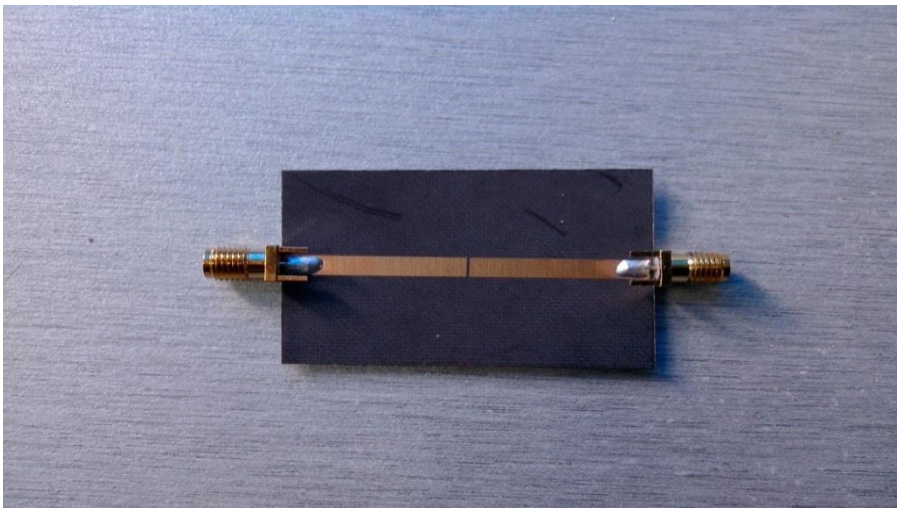

Figure 4.16: Front view of fabricated 900 MHz band pass filter with DGS

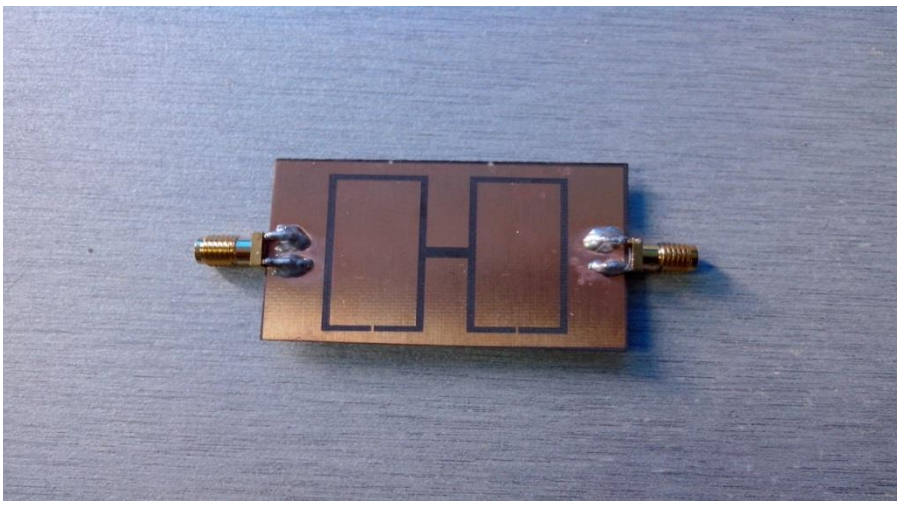

Figure 4.17: Back view of fabricated 900 MHz band pass filter with DGS

Figure 4.16 and 4.17 shows the front view and the back view of the fabricated 900 MHz band pass filter with DGS. The fabrication was based on the simulated design using CST Software. The filter is attached with connectors to ease the connection with RF cable.

As the band pass filter is fabricated and the connectors are attached, later it is tested and measured again using network analyzer in laboratory. Below is the result obtained for parameter S_{11} and S_{21} for the fabricated filter.

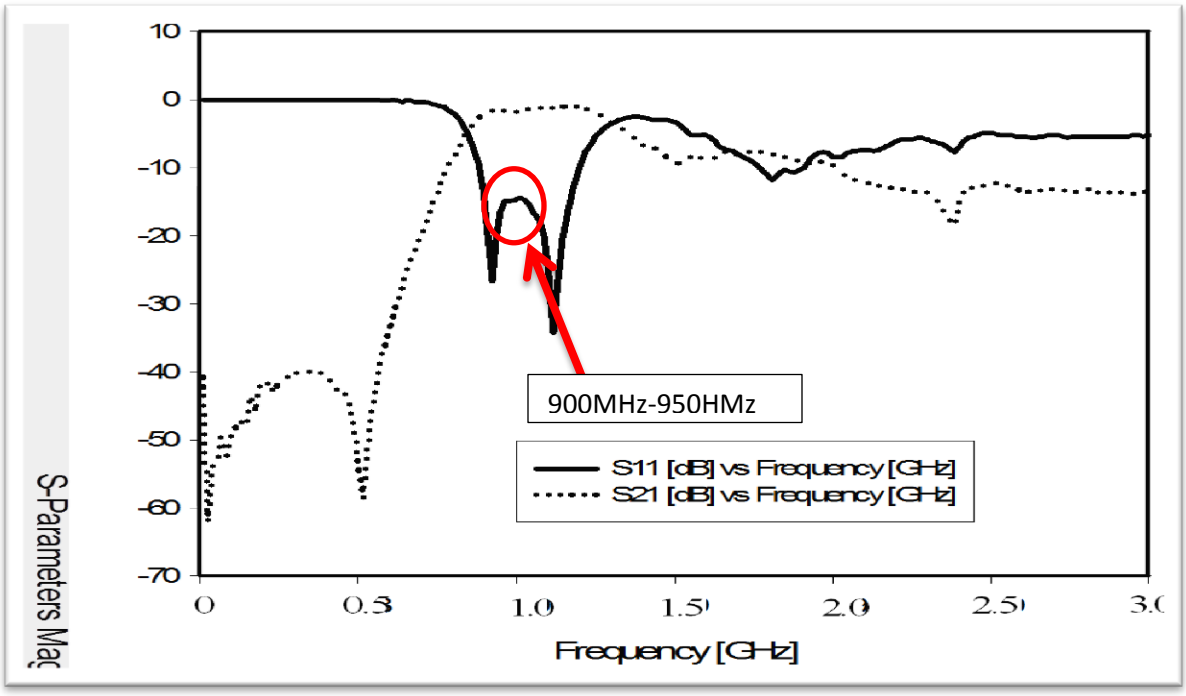

Figure 4.18: Measured result for 900 MHz band pass filter with DGS

Figure 4.18 shows the measured result for the fabricated 900 MHz DGS-BPF. The measured result shows two transmission poles which is same with the simulated result. Based on the result obtained, it clearly shows that the results from simulation and the real measurement are same. The graph curve in the circle is the desired band pass frequency. The allowable range for the frequency is from 900 MHz to 950 MHz. The result obtained has passed the requirement of the first part.

4.5 Energy Harvester Circuit

The second part is the integration of the designed band pass filter with the energy harvester circuit. Energy harvesting is known as micro-energy harvesting, produces small amounts of power from the surrounding environment. Because of this, energy harvester is typically associated with low power applications. While a variety of energy sources can be harvested, open air frequency as RF energy source stands out as a household name. With RF signal increasingly available, the question that begs to be asked would be "Can energy be harvested from open air frequencies?" General opinion would agree that there is indeed energy to be harvested.

4.6 System Overview

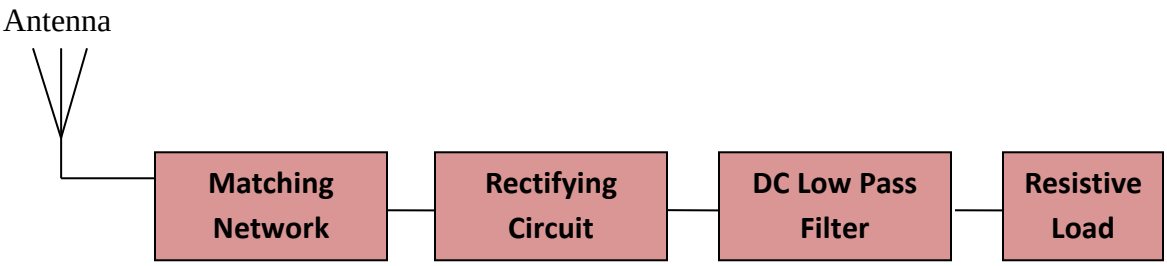

Figure 4.19: Network antenna architecture

A rectenna is a hybrid between a receiving antenna and rectifying circuit that converts RF energy to DC voltage. As shown in Figure 4.19, the energy harvester system is divided into few sections, which are a microwave antenna, a matching circuit and a pre-rectification LPF, rectifying circuit, a post-rectification LPF for DC path and a resistive load.

4.6.1 Matching Network

Matching networks provide a transformation of impedance to a desired value to maximize the energy dissipated by a load. The matching networks ensure that the proper impedance is capture and one such matching method may be a conjugate match of the impedance. RF power captured by the antenna is converted into DC voltage by a diode

and supplied to matching networks. The matching networks will ensure impedance match for optimal power transfer.

4.6.2 Rectifying Circuit

Rectifying is the conversion of alternating current (AC) to direct current (DC). Rectification is performed by a diode that allows current to flow in one direction but nit in the opposite direction. Direct current that has been rectified however has various changes in ripples lingering from the alternating current. Capacitors are used to smooth the current and make it even. Once the signal from matching networks enters rectifying circuit, the current will be converting into DC current from the AC current.

4.6.3 DC Low Pass Filter

A low pass filter is a filter that passes low frequency signals and attenuates signals with frequencies higher than the cutoff frequency. It is basically the opposite of a high pass filter. The signal will be channeled to LPF from rectifying circuit. Here, the signal will be smoothens by suppressing high frequency harmonics present in RF signal.

4.6.4 Resistive Load

Resistive load is the output of the system. Here, the resistive load is the energy harvester board that was used for measurement which is the Powercast P2110-EVAL-02 Energy Harvester Circuit.

4.7 Powercast P2110-EVAL-02 Energy Harvester Circuit

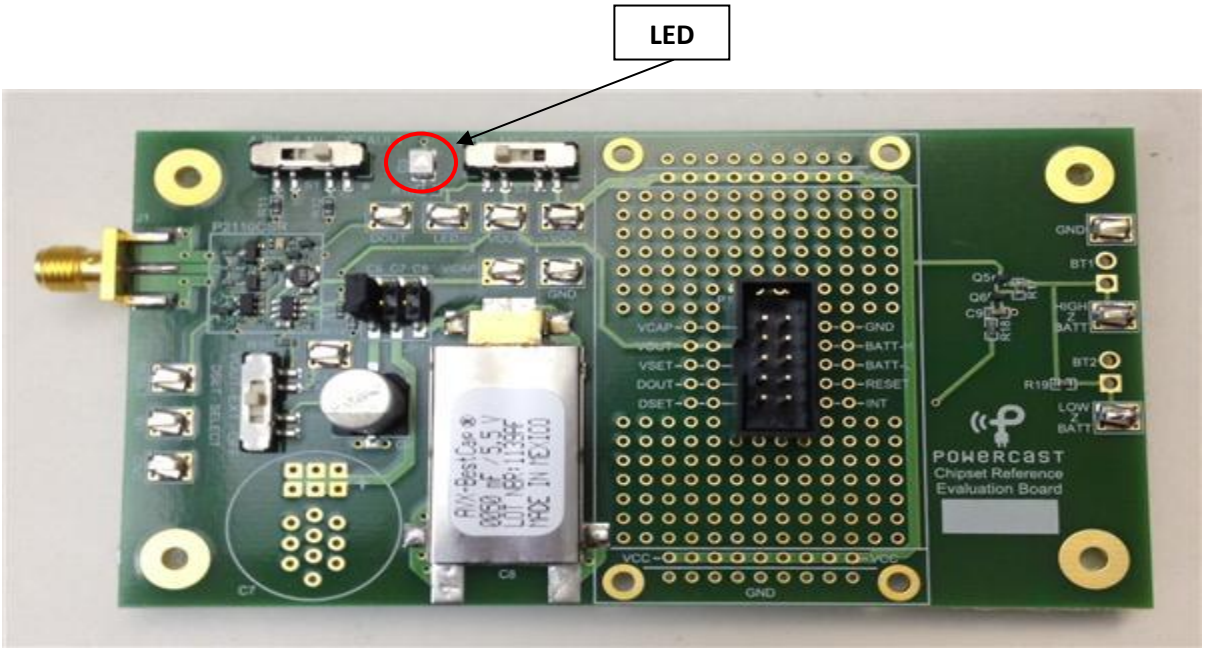

Figure 4.20: Powercast P2110-EVAL-02 Energy Harvester Circuit

Figure 4.20 shows Powercast P2110-EVAL-02 board that was used as energy harvester circuit for this project. This board has an SMA connector to connect the antennas and a 10-pin connector for the charging board. 915 MHz PCB patch antenna is connected with this board.

The type output for this circuit is not fixed which means that it can be determined based on the preference of the user. For example, this circuit gives the flexibility to choose between LED and voltage that can be used to measure as an output. In this project, LED is used as the output signal.

4.8 System Design

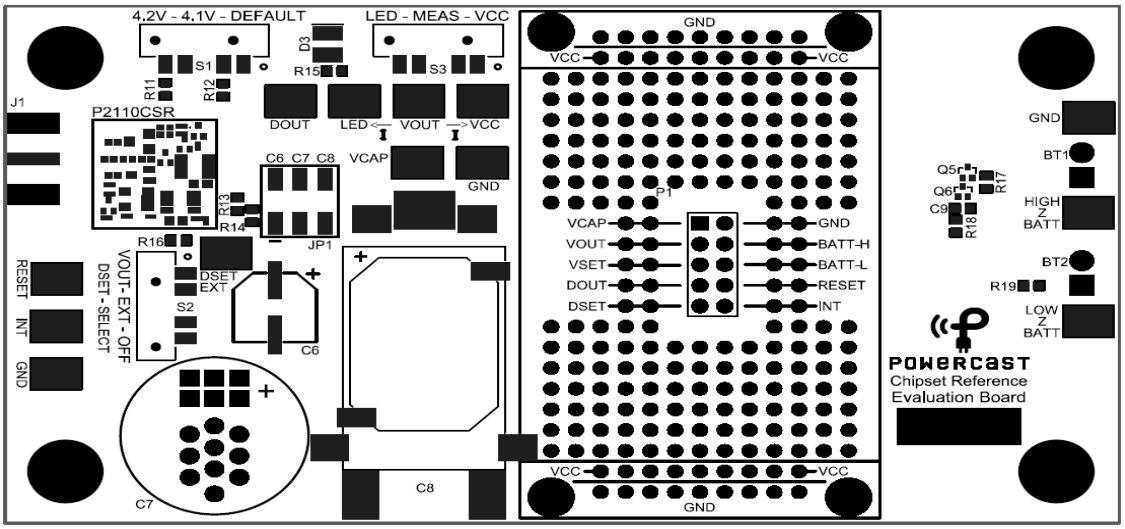

Figure 4.21: Powercast P2110-EVAL-02 Energy Harvester Circuit Design Diagram

Figure 4.21 shows the design and the component of the energy harvester board. Each of the components is important in the board and it has its own function. The entire component is described as per table below

Table 4.3: Component description for Powercast P2110-EVAL-02 Board

Component	Description
BT1, BT2	External battery connection (described in detail below)
C6	Storage capacitor – 1000µF (small)
C7	Storage capacitor – not populated (user determined)
C8	Storage capacitor – 50mF (large)
C9, Q5, Q6, R17, R18	Output switch (described in detail below)
D3	LED for visual indication of power output
J1	SMA connector for antenna or RF input (add DC block for DC short antenna)
JP1	Jumper for selecting storage capacitor C6, C7, or C8
P1	Connector for add-on boards Connector on board: Sullins – P/N: SBH11-PBPC-D05-ST-BK Mating connector: Sullins – P/N: SFH11-PBPC-D05-ST-BK
R11, R12	Resistors for adjusting V_{OUT}, selectable using S1
R13, R14	Resistors for setting V_{OUT} default value
R15	LED bias resistor
R16	Resistor for pulling D_{SET} high using V_{OUT}, selectable using S2
R19	Resistor for limiting current to low impedance batteries
S1	Switch for selecting output voltage (described in detail below)
S2	Switch for D_{SET} selection (described in detail below)
S3	Switch for selecting V_{OUT} load (described in detail below)

The most common part that was used in this project is the GND, V_{out}, LED and the connectors for antenna. Other components are for different function and measurement which does not involve in this project.

4.9 Test Measurement Setup

Procedures

Before starting the real life situation operation, this test measurement should be done first in order to check the functionality of the filter. The band pass filter must be connected with the energy harvester circuit with connectors as in Figure 4.22. The connectors should be tight enough so that there will not be any RF losses. The position of the filter also must be correct so that there will not be any error in the readings.

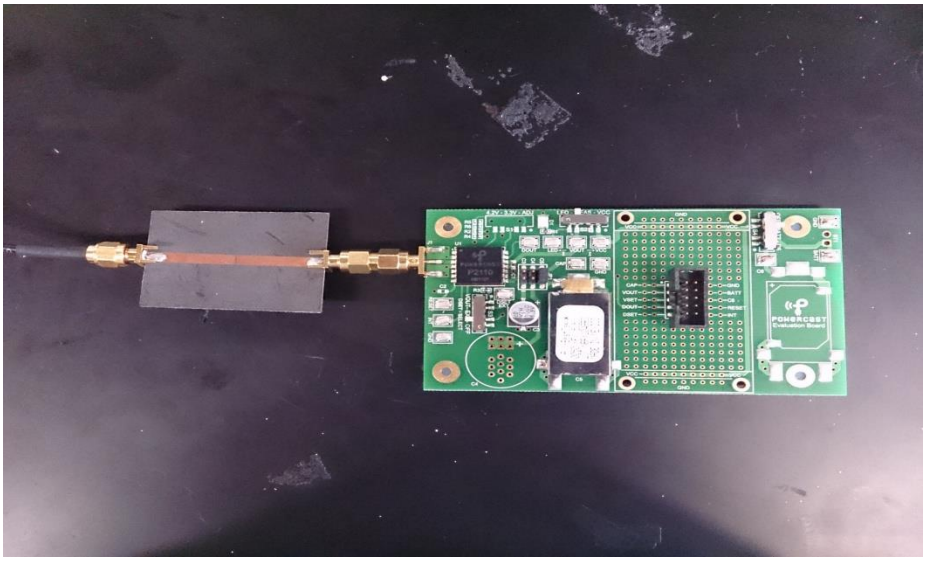

Figure 4.22: Setup of 900 MHz band pass filter with energy harvester circuit

Once the setup is done as in the Figure 4.23, then it must be connected with the signal generators using coaxial cable. The connection also must be tight to prevent any RF losses. All the connection must be correct before the signal generators in turned on.

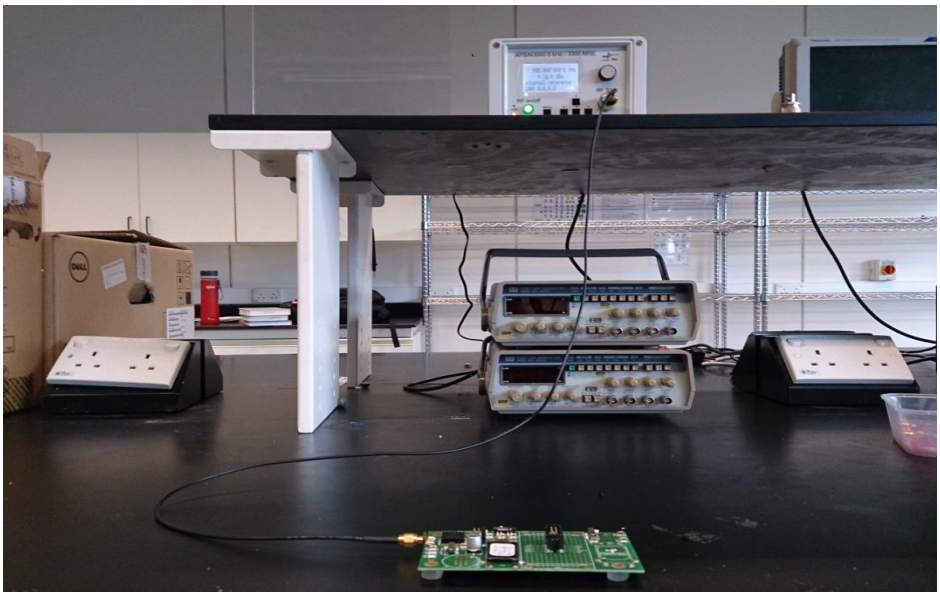

Figure 4.23: The overall setup of the system

Figure 4.23 shows the overall setup of the test measurement process. The signal generator is turned on once all the setup is complete. The frequency range is set from 1500 MHz to 900 MHz as in Figure 4.24 and 4.25. The LED blinking interval time was taken in order to observe any changes.

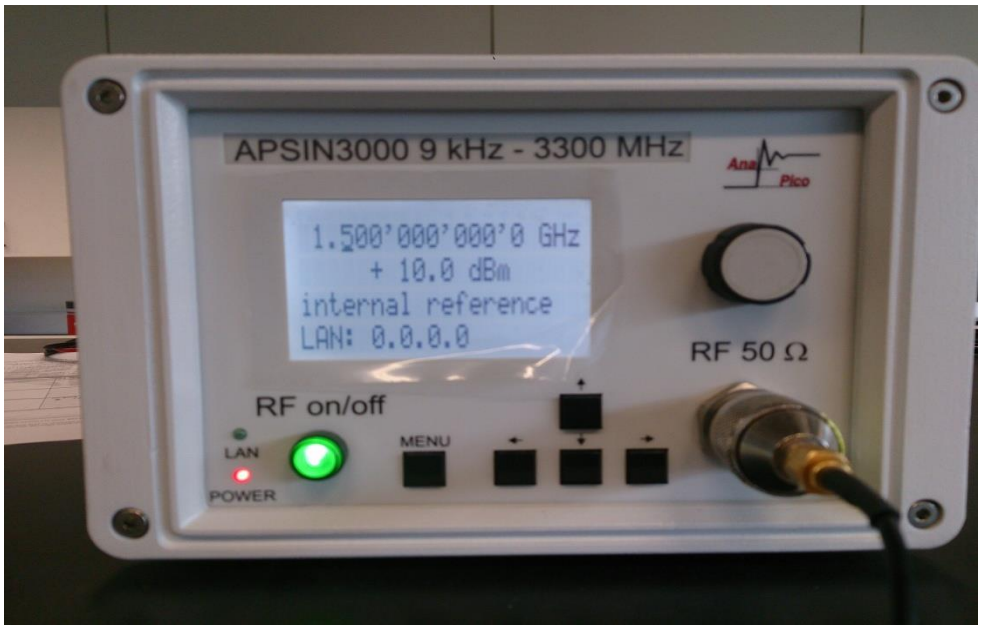

Figure 4.24: 1500 MHz as the input for the system

Figure 4.25: 900 MHz as the input for the system

Once the circuit received its desired frequency, the circuit is turned on and the LED blinks according to its time interval which corresponds to the input frequencies. The radio frequency energy (RF) is converted into DC power and stores it in a capacitor to provide an intermittent, regulated voltage output. The output voltage range is around 1.5 V with 10 dBm which gives us power around 10 mW. The same procedure was repeated but without a band pass filter. The results obtained are tabulated in the table below.

Table 4.4: LED blinking respond based on frequency input without DGS-BPF

Frequency (MHz)	Time for LED to blink (s)
1500	5.97
1400	5.32
1300	4.85
1200	4.02
1100	3.96
1000	3.87
900	3.84

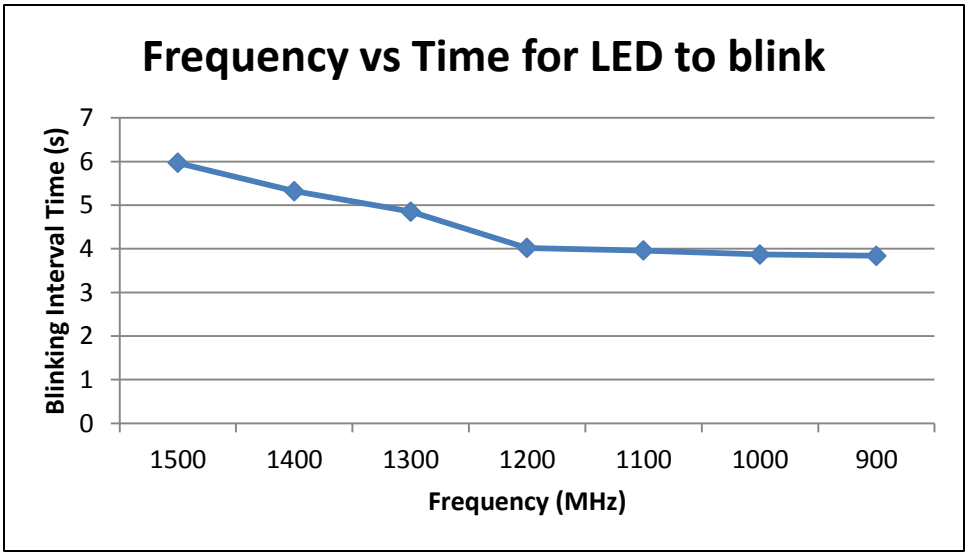

Figure 4.26: Graph without DGS-BPF

Table 4.5: LED blinking respond based on frequency input with DGS-BPF

Frequency (MHz)	Time for LED to blink (s)
1500	4.81
1400	4.36
1300	4.04
1200	3.95
1100	3.82
1000	3.74
900	3.51

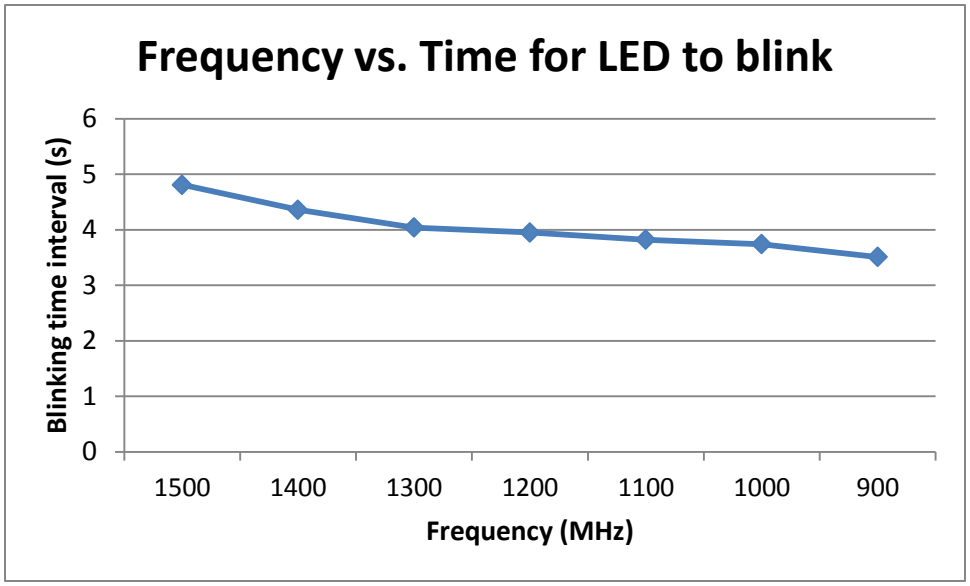

Figure 4.27: Graph with DGS-BPF

From part one, the simulation result and the measured result are the same. This proves that the band pass filter with defected ground structure was designed correctly and accordingly to its parameter. The usage of defected ground structure in the band pass filter is to have an improvement in the return loss. The result also shows that the parameter S_{12} and S_{21} exhibits less than -30 dB and more than -0.5 dB respectively.

In the second part, the designed DGS-BPF filter managed to integrate with the energy harvester circuit. The blinking of LED determines the output of the circuit. From the table and graph above, it shows that as the frequencies decreases, the LED blinking interval time decreases too.

By using the 900 MHz DGS-BPF, a shorter period of blinking time is obtained and other higher frequencies managed to integrate with the energy harvester circuit. Whereas, without using DGS-BPF, the blinking of LED took a longer period of time which indicate that the output voltage is smaller compared with the previous test.

For the final stage, after the test measurement was done, the energy harvester circuit and the DGS-BPF were tested with real life situation. The energy harvester circuit was connected with an antenna of 915 MHz and 6.1 dBi. A transmitter was used to transmit frequency with a range from 915 MHz to 1000 MHz.

The first setup was without DGS-BPF as showed in Figure 4.28. The output voltage was measured by changing the distance of transmitter and the energy harvester circuit. The same procedures were repeated with the integration of DGS-BPF and energy harvester circuit as in Figure 4.29. The setup of the system and the results obtained are recorded.

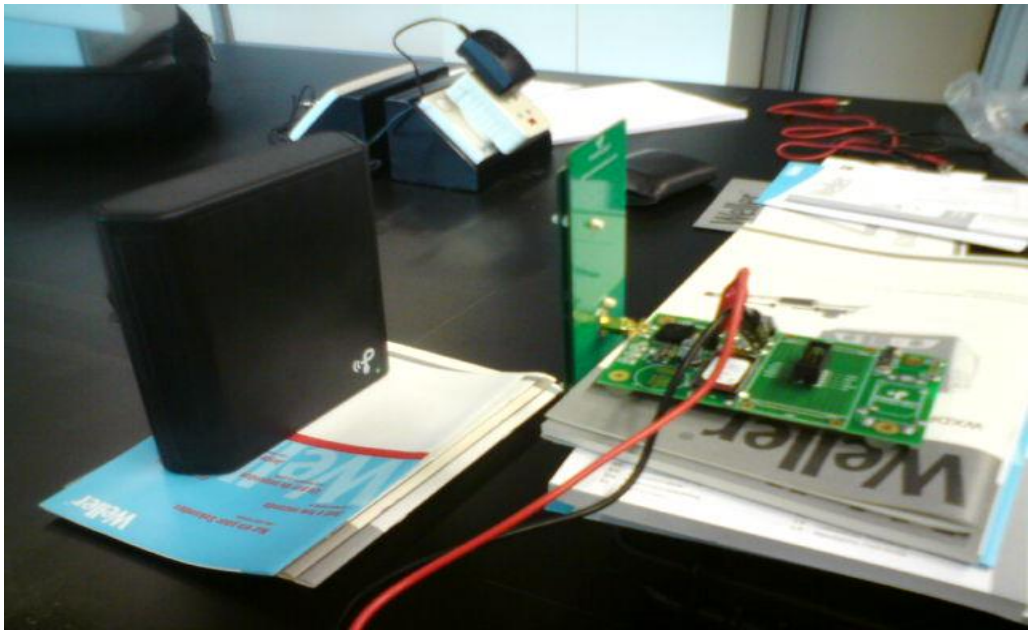

Figure 4.28: The setup of transmitter and energy harvester circuit without DGS-BPF

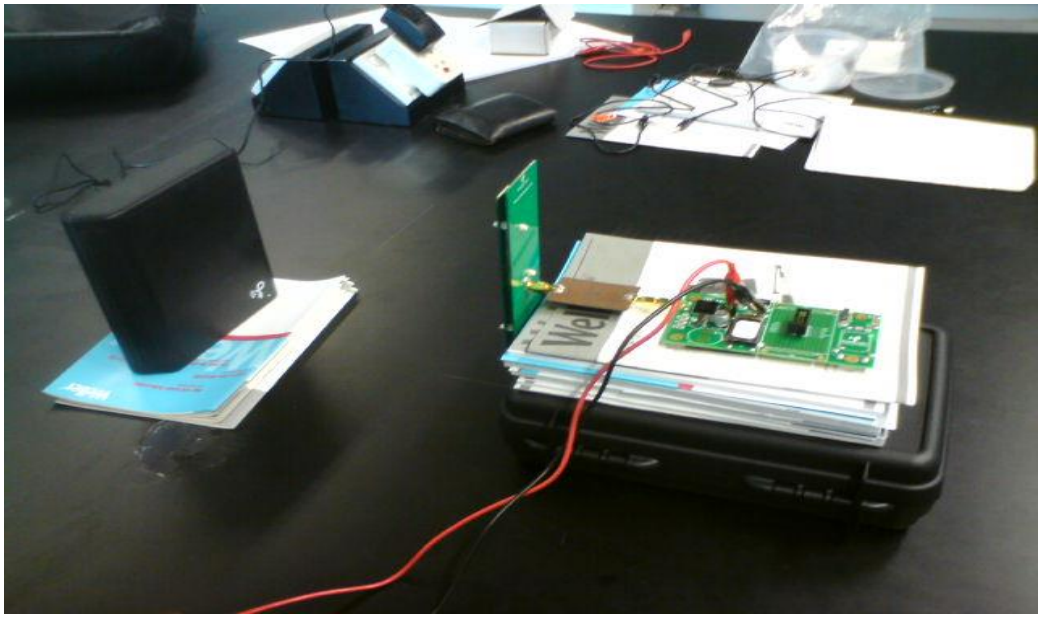

Figure 4.29: The setup of transmitter and energy harvester circuit with DGS-BPF

Table 4.6: Result of energy harvester circuit with antenna and transmitter

Without DGS-BPF		With DGS-BPF	
Distance from Tx (m)	Output voltage (v)	Distance from Tx (m)	Output voltage (v)
0.15	3.49	0.15	3.49
0.30	3.36	0.30	3.36
0.45	3.21	0.45	3.27
0.60	3.07	0.60	3.15
0.75	2.95	0.75	3.01
0.90	2.76	0.90	2.96
1.00	2.59	1.00	2.83

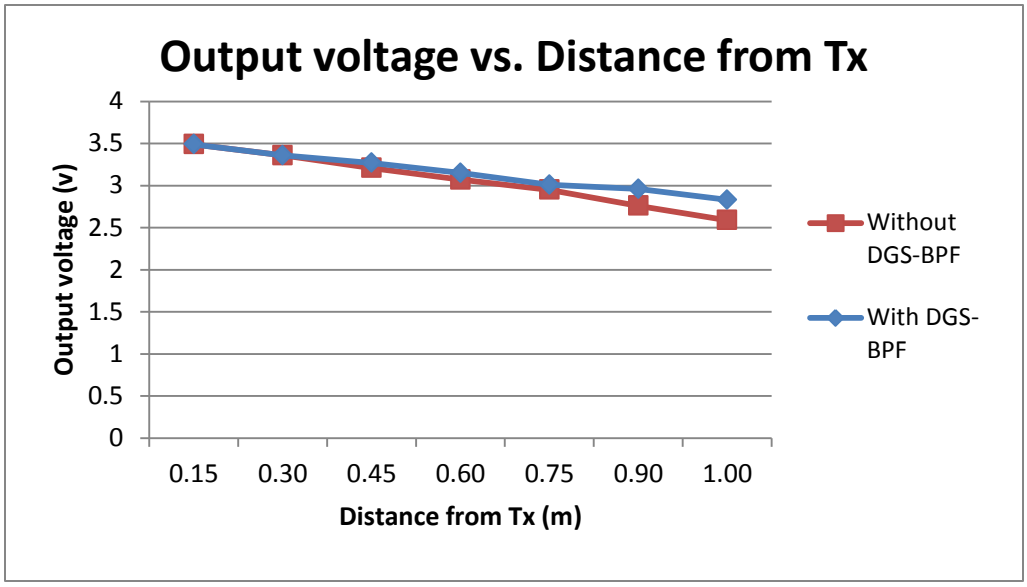

Figure 4.30: Graph of output voltage vs. distance from transmitter (Tx)

From the results obtained above, it shows that the output voltage for both sets of setup decreases as the distance from the transmitter increases. This is because once the distance increases, the antenna will experience difficulties to receive the signal from the transmitter, thus this will decreases the output voltage produce by the circuit. But from comparison between two sets, the set with DGS-BPF gives a better trend of voltage reading as it does not decrease abruptly. Therefore, it is clearly proven that the project is successfully implemented and the analysis was done based on the results.

CHAPTER 5
CONCLUSION AND RECOMMENDATION

The integration of band pass filter with the energy harvester circuit was successfully carried out. Using frequency as an input to the band pass filter, connection was made to the energy harvester circuit. An output of DC voltage is obtained and this proved that the objective of this project has been achieved.

With the usage of DGS in the filter, it helps to reduce the size of the filter, and this indirectly can reduce the cost of designing it. This is because there will be no extra or complex design of filters needed. Besides that, a better sharpness of stop band also can be achieved by using DGS in the filter and by this, the output of the filter will be better and can be used for other application such as the energy harvester circuit.

Many improvements can be done in the future, such as designing a band pass filter with a simpler design. It is not necessary for the band pass filter to be in the same design as in this project paper. Besides that, the usage of software also can be improved. A newer version of software would give a faster results and this will save more time in designing the filters.

This system can be used in daily life and it will be very useful in saving energy. We can used open air frequencies to produce a small current and improvement can be done in the circuit to obtain a higher current value to be used for a higher current consumption load in the future. Furthermore, this application also can be used for replacing batteries. It is really hard to charge batteries all the time, thus by implementing this idea in a wider scope, a good resolution can be obtained.

By completing this project, it is really hoped that microwave communication will be a common way of interaction and provide comfort in our daily life.

CHAPTER 6
REFERENCES

[1] L. Haiwen, Z. Zhichong, G. Xuehui, and J. Shan, "A bandpass filter based on fractal shaped defected ground structure resonators for wireless communication," in *Microwave and Millimeter Wave Technology (ICMMT), 2010 International Conference on*, pp. 201-203, 2010.

[2] H. Pai-Yi, W. Ro-Min, and C. Yin-Hsin, "A Miniaturized Dual-Band Bandpass Filter Using Open-Loop and SIR-DGS Resonators," in *Silicon Monolithic Integrated Circuits in RF Systems, 2008. SiRF 2008. IEEE Topical Meeting on*, pp. 191-194, 2008.

[3] K. Chul-Soo, P. Jun-Seok, A. Dal, and J.-B. Lim, "A novel 1-D periodic defected ground structure for planar circuits," *Microwave and Guided Wave Letters, IEEE,* vol. 10, pp. 131-133, 2000.

[4] W. Bian, L. Chang-Hong, Q. Pei-Yuan, and L. Qi, "Compact Dual-Band Filter Using Defected Stepped Impedance Resonator," *Microwave and Wireless Components Letters, IEEE,* vol. 18, pp. 674-676, 2008.

[5] V. Radisic, Q. Yongxi, R. Coccioli, and T. Itoh, "Novel 2-D photonic bandgap structure for microstrip lines," *Microwave and Guided Wave Letters, IEEE,* vol. 8, pp. 69-71, 1998.

[6] H. B. El-Shaarawy, F. Coccetti, R. Plana, M. El-Said, and E. A. Hashish, "A novel reconfigurable DGS cell for multi-stopband filter on CPW technology," in *Microwave Conference, 2008. APMC 2008. Asia-Pacific*, pp. 1-4, 2008.

[7] S. Singh and B. Rawat, "DGS based SIR filters for wireless communication on anisotropic substrate," in *Microwave Conference, 2006. APMC 2006. Asia-Pacific*, pp. 1144-1153, 2006.

[8] H. Liu, Z. Li, and X. Sun, "Compact defected ground structure in microstrip technology," *Electronics Letters,* vol. 41, pp. 132-134, 2005.

[9] T. Sio-Weng, K.-W. Tam, and R. P. Martins, "Compact Microstrip Quasi-Elliptic Bandpass Filter Using Open-Loop Dumbbell Shaped Defected Ground Structure,"

in *Microwave Symposium Digest, 2006. IEEE MTT-S International*, pp. 527-530, 2006.

[10] D. M. Pozar, *Microwave Engineering*, Second Edition, Wiley and Sons, 1998.

[11] R. E. Collin, *Foundation for Microwave Engineering*, Second Edition, McGraw Hill, 1992.

[12] R. Garg, P. Bhartia, I. Bahl, and A. Ittipibon, Microstrip Antenna Design Handbook, Artech House, Boston, London, 2001.

[13] D. M. Pozar, "A review of bandwidth enhancement techniques for Microstrip antennas, In microstrip antennas," *IEEE Press*, New York, 1995.

[14] D. H. Schaubert and F. G. Farrar, "Some conformal printed circuit antenna design," *Proc. Workshop Printed Antenna Technology*, New Mexico State University, Las Cruces, NM, pp. 5/1-5/21, Oct. 1979.

[15] G. Kumar and K. C. Gupta, "Directly coupled multiple resonator wide-band Microstrip antennas," *IEEE Trans. On Antennas and Propagation*, vol. 33, No.6, pp. 588-593, 1985.

[16] C. H. Tsao, Y. M. Hwang, F. Kilburg and F. Dietrich, "Aperture-coupled patch antennas with wide bandwidth and dual polarization capabilities," *IEEE Antennas and Propagation Symp. Digest*, pp. 936-939, 1988.

[17] A. Ittipiboon, B. Clarke and M. Cuhaci, "Slot-coupled stacked Microstrip antennas," *IEEE Antennas and Propagation Symp. Digest*, pp. 1108-1111, 1990.

[18] F. Croq and D. M. Pozar, "Millimeter-wave design of wide-band aperture coupled stacked Microstrip antennas," *IEEE Trans. On Antennas and Propagation*, vol. 39, No. 12, pp. 1770-1776, 1991.

[19] S. D. Targonski, R. B. Waterhouse and D. M. Pozar, "Millimeter-wave design of wideband aperture-coupled stacked Microstrip antennas," *IEEE Trans. On Antennas and Propagation*, vol. 46, No. 9, pp. 1245-1251, 1998.

[20] D. Heberling et al., "Simple feeding technology for stacked Microstrip antennas," *in Proceedings 19th European Microwave Conference, London*, UK , pp. 155-160, September 1989.

[21] R. T. Cock and C. G. Christodoulu, "Design of a two-layer capacitive coupled microstrip patch antenna element for broadband applications," *IEEE, AP(S)*, pp. 936-939, 153, 1987.

[22] F. Croq, "Stacked resonators for bandwidth enhancement: A comparison of two feeding techniques," *IEE Proceedings*, Part H, vol. 140, No. 4, pp. 303-309, 1993.

[23] J. P. Damiano et al. "Study of multiplayer Microstrip antennas with radiating elements of various geometry," *IEEE Proceedings*, Part H, vol. 137, No. 3 , pp. 163-170, 1990.

[24] S. Yano and A. Ishimaru, "Broadbanding of Microstrip antennas by orthogonal polarizations," *IEEE Antennas and Propagation Symp. Digest*, pp. 363-365, 1981.

[25] Y. L. Chow, Z. N. Chen, K. F. Lee, and K. M. Luk, "A design theory on broadband patch antennas with slot," *IEEE, AP(S)*, pp. 1124-1127, 1998.

[26] T. Huynh and K. F. Lee, "Single-layer single patch wideband Microstrip antenna," *Electron. Lett.*, vol. 31, pp. 1310-1312, 1995.

[27] K. F. Lee, K. M. Luk, K. F. Tong, S. M. Shum, T. Huynh, and R. Q. Lee, "Experimental and simulation studies of coaxially fed U-slot rectangular patch antenna," *Inst. Elect. Eng. Proc. Microwave Antennas Propagat.*, 144, pp. 354-358, 1997.

[28] R. Bahalla and L. Shafai, "Resonance behavior of single U-slot Microstrip patch antenna," *Microwave Opt. Technol. Lett.*, vol. 32, No. 5, pp. 333-335, 2002.

[29] G. Dubost, Flat radiating dipoles and applications to arrays, Research studies press, New York, 1981.

[30] H. F. Pues and A. R. Van de Capelle, "An impedance matching technique for increasing the bandwidth for microstrip antennas," *IEEE Transactions on Antennas and Propagation*, vol. 37, No. 11, pp. 1345-1354, 1989.

[31] D. A. Paschen, "Practical examples of integral broadband matching of Microstrip antenna elements," *Proc. Antenna Applications Symp.* pp. 199-217, 1986.

[32] N. Herscovici, "A wideband single layer patch antenna," *IEEE Transactions on Antennas and Propagation*, vol. 46, No. 4, pp. 471-474, 1998.

[33] K. L. Wong and Y. F. Lin, "Microstrip line fed compact Microstrip antenna with broadband operation," *IEEE Antennas and Propagation Symp. Digest*, pp. 1120-1123, 1998.

[34] K. R. Carver and J. W. Mink, "Microstrip antenna technology," *IEEE Trans. On Antennas and Propagation*, vol. Ap-29, pp. 2-24, Jan. 1981.

[35] D. M. Pozar, "Microstrip antenna aperture coupled to a microstrip line," *Electron. Lett*, vol. 21, pp. 49-50, Jan. 1985.

[36] J-F. Zürcher, F. Gardiol, "Broadband Patch Antennas," Artech House, 1995.

[37] F. Croq and A. Papiernik, "Large Bandwidth Aperture-Coupled Microstrip Antenna," *Electronics Letters*, 26, pp. 1293-1294, August 1990.

[38] G. S. Kirov, A. Abdel-Rahman and A. S. Omar, "Wideband Aperture Coupled Microstrip Antenna," *IEEE, AP-S*, vol. 2, *2003*.

[39] R. Q. Lee, K. F. Lee and J. Bobinchack, "Characteristics of a two layer electromagnetically coupled rectangular microstrip antenna," *Electron. Lett.*, vol.23, no. 20, pp.1017-1072, Sept.1987.

[40] N. Alexopoulos and D. Jackson, "Fundamental superstrate (cover) effect on printed Circuit Antennas," *IEEE Transactions on Antennas and Propagation*, vol. Ap-32, pp. 807-816, Aug. 1984.

[41] Y. Sugio, T. Makimoto, S. Nishimura, and H. Nakanishi, "Analysis for gain enhancement of multiple-relection line antenna with dielectric plates," *IEEE Trans. IECE*, pp. 80-112, Jan. 1981.

[42] D. Jackson and N. Alexopoulos, "Gain Enhancement Methods for Printed Circuit Antennas," *IEEE Transactions on Antennas and Propagation*, vol. AP-33, no. 9, pp. 976-987, Sep. 1985.

[43] H. Yang and N. Alexopoulos, "Gain Enhancement Methods for Printed Circuit Antennas through Multiple Superstrates," *IEEE Transactions on Antennas and Propagation*, vol. AP-35, no. 7, pp. 860-863, July 1987.

[44] D. Jackson and A. Oliner, "A Leaky–wave Analysis of the High Gain Printed Antenna Configuration," *IEEE Transactions on Antennas and Propagation*, vol. AP-36, no. 7, pp. 905-909, July 1988.

[45] F. Zavosh and James T. Aberle, "Design of high gain microstrip antenna," *Microwave Journal,* vol. 42, No. 9, pp. 138-148, Sept. 1999.

[46] A. Abdel-Rahman, A. K. Verma, G. S. Kirov and A. S. Omar, "Aperture Coupled Microstrip Antenna With Quasi-Planner Surface Mounted Horn," *in Proceedings 33th European Microwave Conference, Munich*. pp.1377-1380, Oct. 2003.

[47] A. Abdel-Rahman, A. K. Verma and A. S. Omar, "Gain Enhancement of Microstrip Antenna Array Using Surface Mounted Horn," *in Proceedings 34th European Microwave Conference, Amsterdam*. pp. 1377-1380, Oct. 2003.

[48] D. Ahn et al, "A Design of the Low-pass Filter using the Novel Microstrip Defected Ground Structure," *IEEE Trans. Microwave Theory Tech.,* vol. 49, No. 1, pp. 86-91, Jan. 2001.

[49] F.R. Yang, Y. Qian and T. Itoh, "A novel uni-planar compact PBG structures for filter and mixer applications," *IEEE Microwave Theory Tech. Symposium, MTT (S),* pp. 919-922, 1999.

[50] J.S. Lim, C.S. Kim, Y.K. Lee, D. Ahn and S. Nam, "A spiral-shaped defected ground plane structure for coplanar Waveguide," *IEEE Microwave Wireless component Lett.,* vol.12, no. 9, pp. 330-312, Sept. 2002.

[51] W. Schwab, F. Boegelsack, and W. Menzel " Multilayer suspended stripline and coplanar line filters," *IEEE Trans. Microwave Theory Tech.*, vol. 42, pp. 1404-1407, July 1993.

[52] C. Quendo, E. Rius, C. Person, and M. Ney, " Integration of optimized low-pass filters in a band pass filter for out-of-band improvement," *IEEE Trans. Microwave Theory Tech.*, vol. 49, pp. 2376-2383, Dec. 2001.

[53] T. Kim and C. Seo, "A Novel Photonic Bandgap Structure for Low-pass Filter of Wide Stop band," *IEEE Microwave and Guided Wave Letters*, vol. 10, No. 1, pp. 13-15, Jan. 2000.

[54] C. Kim, et al, "A Novel 1-D Periodic Defected Ground Structure for Plane on Circuits," *IEEE Trans. Microwave and Guided Wave Letters*, vol. 10, No. 4, pp. 131-133, Apr. 2000.